

FREQUENCY DOMAIN METHODS FOR ANALYZING THE CLOSED-LOOP
DIRECTIONAL STABILITY AND MANEUVERABILITY
OF DRIVER/VEHICLE SYSTEMS

Charles C. MacAdam
The University of Michigan
Transportation Research Institute
Ann Arbor, Michigan 48109, USA

*Proceedings of the International Conference on Modern Vehicle
Design Analysis, London UK, June 1983.*

ABSTRACT

Several frequency domain methods useful for describing and analyzing the directional stability and maneuverability of the closed-loop system comprised of the driver and vehicle are examined. In particular, Bode plots, Nyquist diagrams, and Nichols charts are illustrated and compared. The utility and specific features of each method for analyzing driver/vehicle responses are demonstrated through examples using experimental measurements of driver/vehicle interactions and mathematical simulation. A principal conclusion, based upon the analysis techniques and example calculations, is that preview-based steering control strategies typically employed by drivers of automobiles may produce a tradeoff of closed-loop directional stability in exchange for path maneuverability.

INTRODUCTION

This paper presents and illustrates several frequency domain methods useful for describing and analyzing the directional stability and maneuverability of the closed-loop system comprised of the driver and vehicle. Three particular methods commonly employed in control system analyses are discussed and compared. The three analysis techniques examined are: a) Bode plots, b) Nyquist diagrams, and c) Nichols charts. The advantages/disadvantages and particular utility of each method for analyzing driver/vehicle responses are illustrated through examples based on experimental measurements of driver/vehicle interactions and mathematical simulation.

The paper begins with a brief introductory review of each method. Driver/vehicle experimental measurements are then presented to illustrate the appearance or locus of such measurements on plots/diagrams corresponding to each of the above techniques. Following an interpretation and discussion of the experimental data presented on these plots, analogous "data" derived from a mathematical model to illustrate more extreme variations in vehicle and driver characteristics are presented and discussed in similar fashion. Finally, the topic of driver/vehicle maneuverability, as it is influenced by driver control characteristics and vehicle directional dynamics, is examined and discussed. The trade-off or compromise between closed-loop system stability and maneuverability is demonstrated through frequency domain analysis and computer simulation calculations.

REVIEW OF THREE FREQUENCY DOMAIN ANALYSIS TECHNIQUES

A summary of three particular methods applicable to analyzing driver/vehicle data within the frequency domain is briefly introduced in this section. Specific examples of how these techniques may be applied to driver/vehicle frequency response measurements and computer simulation calculations are presented in the remainder of the paper.

Bode Method

The Bode plot, or frequency response plot as it is commonly referred to, simply consists of the gain and phase of a transfer function plotted as a function of sinusoidal input frequency. This type of plot is by far the most common form used for representing data in the frequency domain. Several "rules of thumb" exist for interpreting data presented in this format, particularly with regard to determining stability of closed-loop control systems. As will be shown for some of the driver/vehicle data presented in this paper, application of such "rules of thumb" for determining the stability of the closed-loop driver/vehicle system can sometimes be misleading and should be employed with caution. A more rigorous and precise method for determining the stability of such systems is available through the use of Nyquist diagrams.

Figure 1 shows an example Bode plot for a set of driver/vehicle measurements as might be obtained from a certain type of closed-loop disturbance test. The frequency response seen here would typically represent the transfer function of the combined driver/vehicle system identified by an experimental procedure in which a disturbance input is applied to the steering system during straight-line regulatory driving. This type of experimental test is the basis for much of the frequency response data presented in this paper and is described more fully in the next section.

The two most common descriptors of driver/vehicle frequency response characteristics (and Bode plots in general) are: 1) crossover frequency and 2) phase margin. Crossover frequency is defined as that frequency at which the transfer function gain is equal to unity (0 db). Phase margin is defined as the difference between the phase angle occurring at the crossover frequency and 180 degrees. (See Figure 1.) For typical driver/vehicle data presented in this form, the crossover frequency is often used as an approximate measure of the system bandwidth. The amount of phase margin generally reflects the degree of closed-loop system damping and hence stability (e.g., zero phase margin implies a neutrally stable system). In fact, the primary "rule of thumb" for interpreting the stability of driver/vehicle data displayed on a Bode plot is to equate increased phase margin with increased stability. While this "rule of thumb" succeeds far more often than it fails, an example of how it can fail to accurately portray the stability of a closed-loop system is illustrated in a later section.

Nyquist Method

The simple block diagram of Figure 2 depicts a closed-loop system achieved by a single-loop closure about the open-loop transfer function, $y/e = Y_o$. Such a diagram could be used to represent, in a very elementary form, a driver/vehicle directional control system. The closed-loop transfer function relating y to x is given by

$$y/x = Y_o / (1 + Y_o) \quad (1)$$

Figure 1. Example Bode Plot

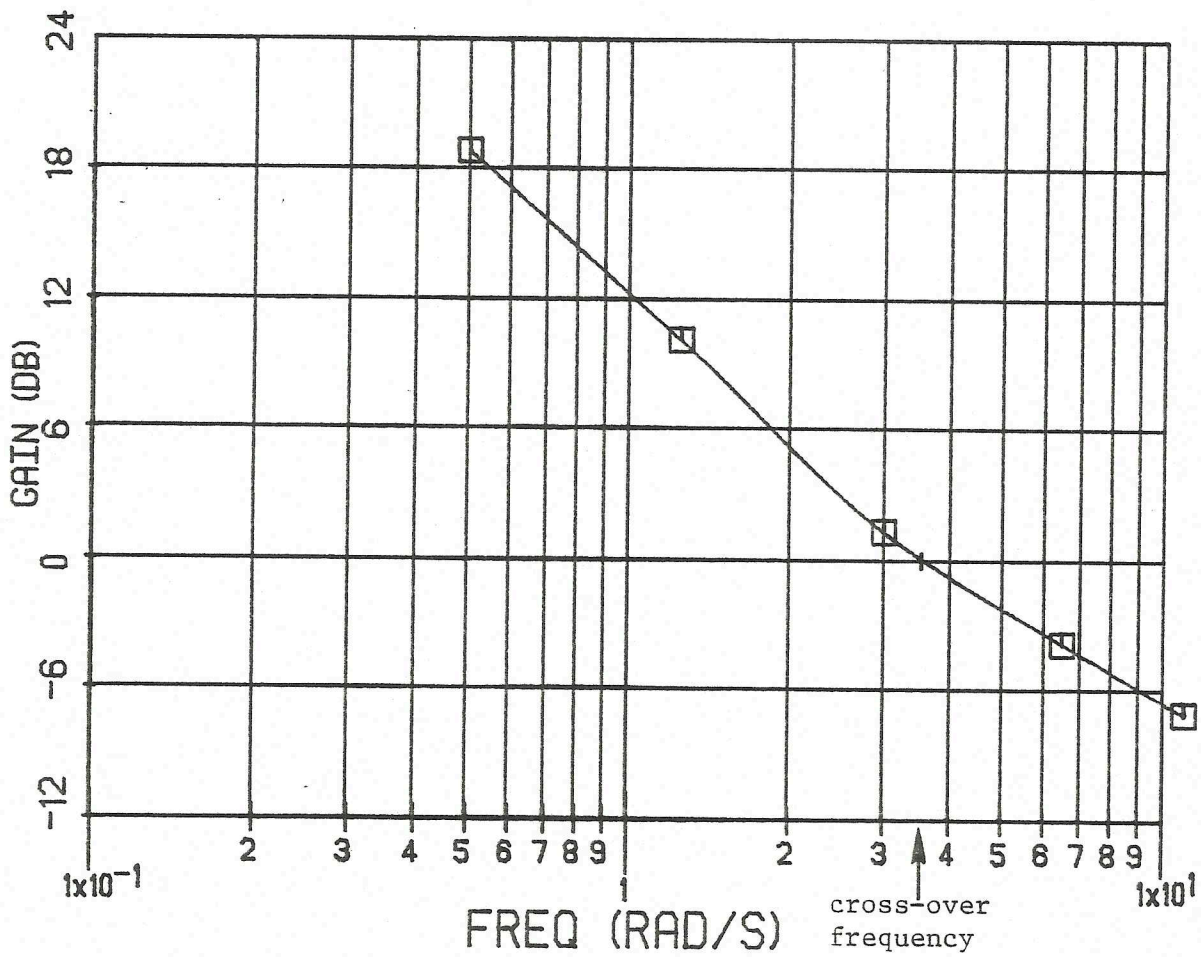
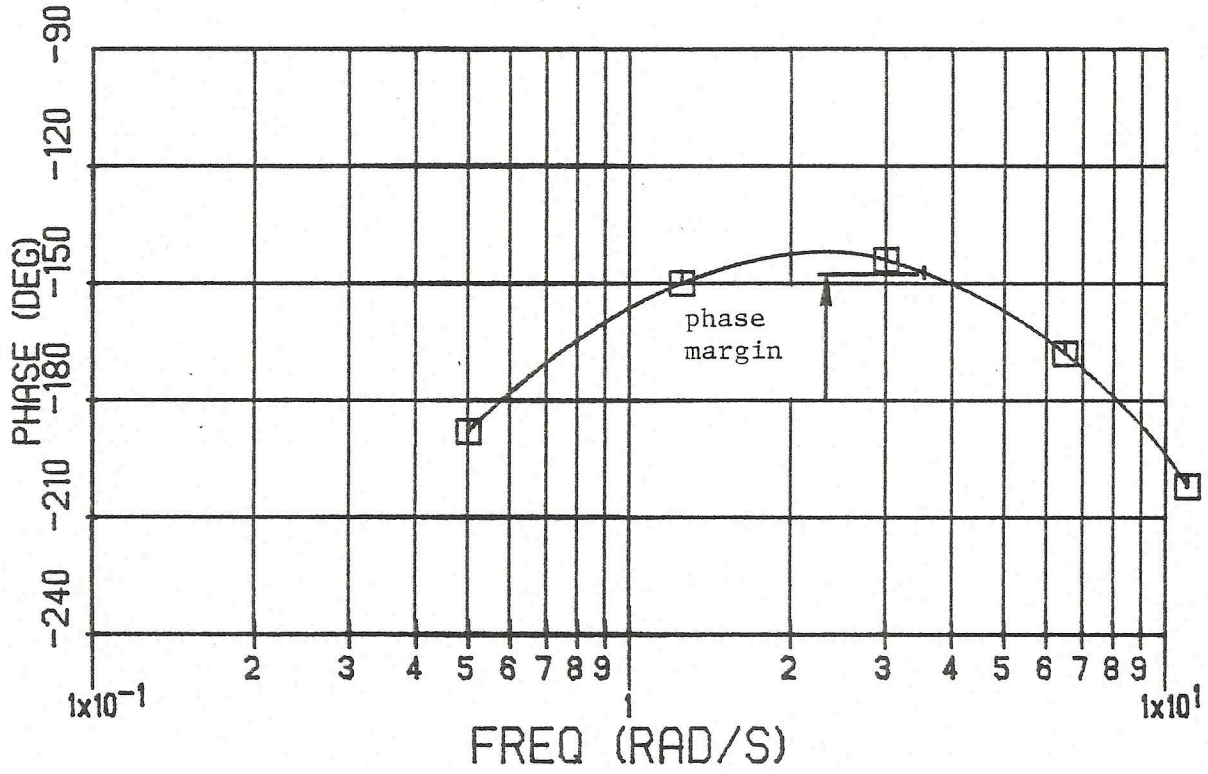
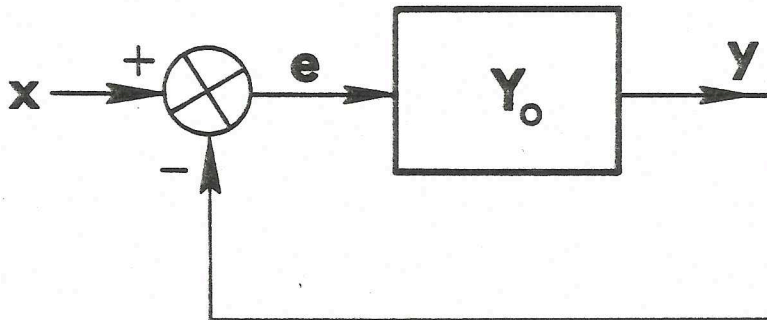


Figure 2. Simple Closed-Loop Control System



Stability of the closed-loop system is, of course, determined by the roots of $1 + Y_0$. The Nyquist stability criterion (James, Nichols, and Phillips, 1947) provides an alternate graphical method for determining closed-loop stability by examination of the complex-plane plot of $1 + Y_0$. Stated concisely, the system is stable if the number of counter-clockwise rotations of $|1 + Y_0|$ about the origin is equal to the number of poles of $(1 + Y_0)$ with positive real parts minus the number of zeroes of $(1 + Y_0)$ with positive real parts.

Application of the Nyquist diagram here is not primarily of interest for determining whether or not a driver/vehicle system is stable, but rather, for determining the degree of stability (or resonance) present. That is, it is assumed here that the closed-loop system is stable and the basic intent is to evaluate its degree of stability, possibly contrasting/comparing it with another system.

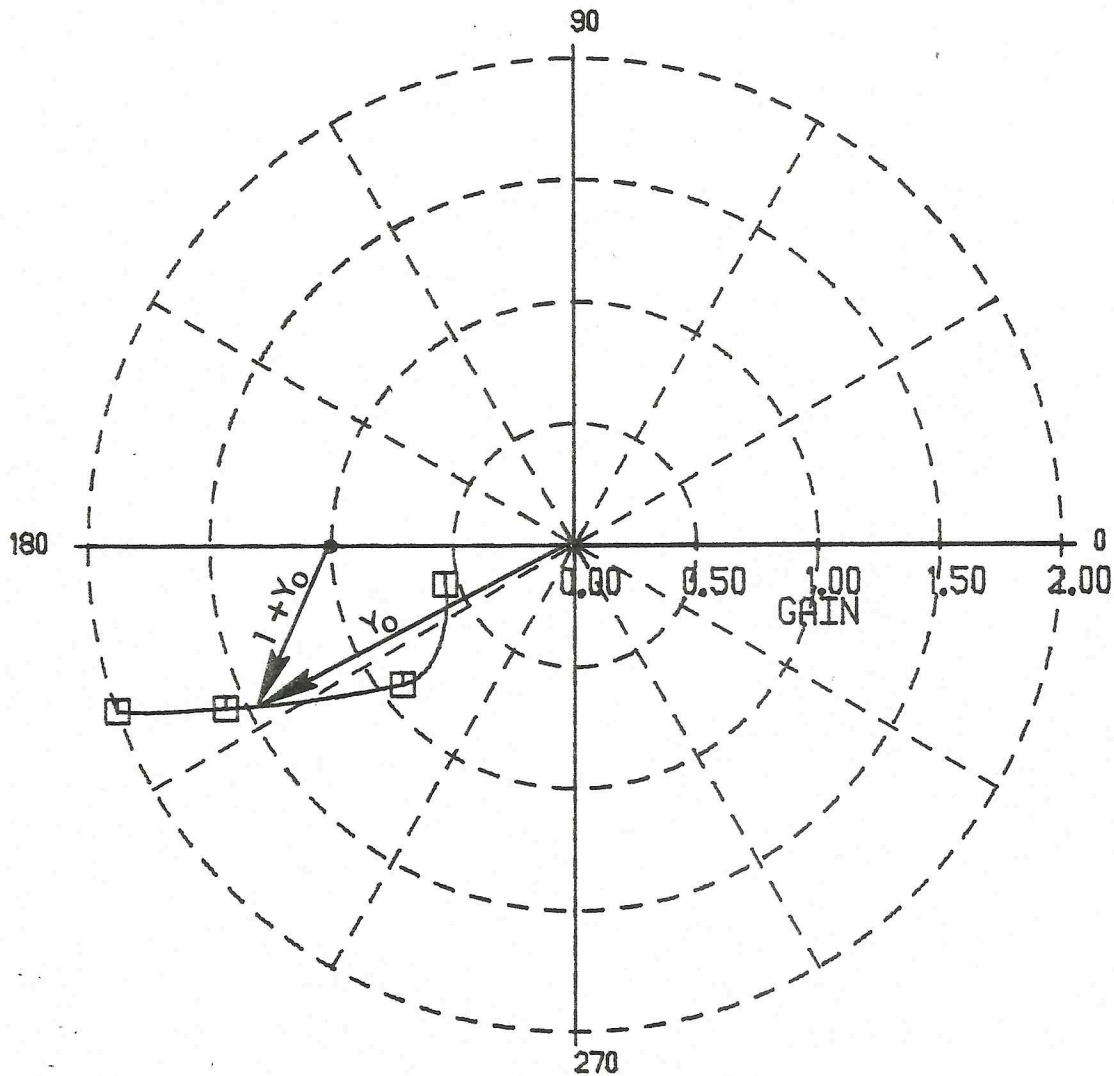
The Nyquist diagram, or complex-plane plot of $1 + Y_0$, can be obtained by simply plotting Y_0 and then displacing the plot one unit to the right, or, more simply, plotting Y_0 and displacing the origin one unit to the left (see Figure 3). The $(-1,0)$ point then becomes the so-called critical point, rather than the origin. Most Nyquist diagrams (and those appearing in later sections of this paper) are displayed in polar coordinate form, the polar radius equated with $|Y_0|$, and polar angle equated with the phase angle of Y_0 . Hence the critical point becomes $(1,180 \text{ degrees})$ in polar form.

Examination of the above equation and Figure 3 reveals that the degree of resonance of the closed-loop system is given by

$$M = |Y_0| / |1 + Y_0| \quad (2)$$

or, the ratio of the magnitudes of the two vectors shown in Figure 3. The degree of resonance increases as the Y_0 plot approaches more closely to the $(1,180 \text{ degree})$ critical point. A locus of Y_0 which passes through the $(1,180 \text{ degree})$ point of course exhibits infinite resonance and reflects neutral stability for the closed-loop system. The value of maximum resonance is commonly used as a direct measure of the stability of the closed-loop system. The topic of M-circles, contained in most control system textbooks, provides a convenient means of identifying the closed-loop system resonance from Nyquist diagrams.

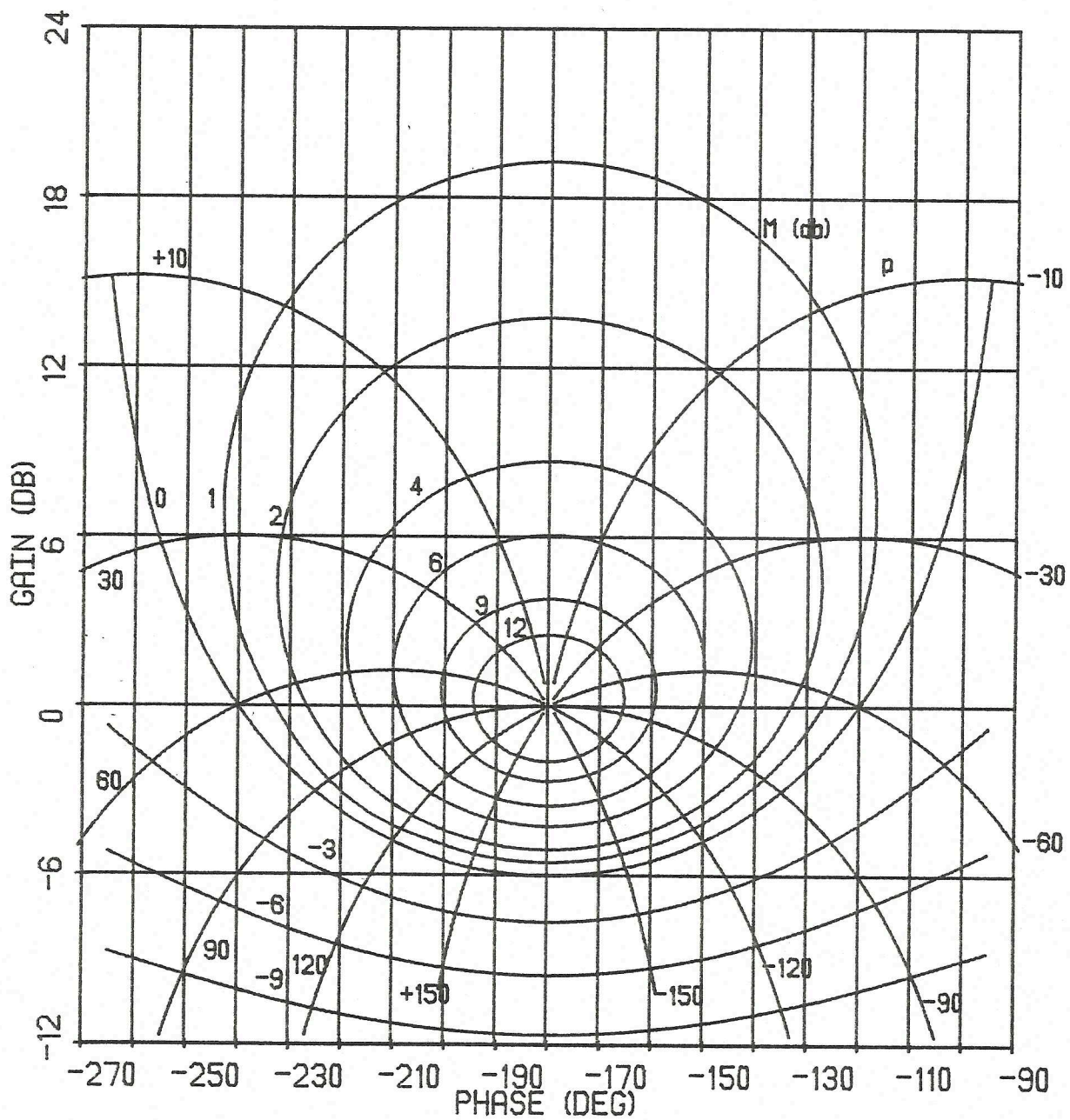
Figure 3. Example Nyquist Diagram



Nichols Chart

The Nichols chart (James, Nichols, and Phillips, 1947; D'Azzo and Houpis, 1981) is simply a graphical "mapping" technique which relates the gain and phase of the open-loop transfer function, Y_0 , to the gain and phase of the closed-loop transfer function, $Y_0/(1 + Y_0)$, at any frequency. The equations describing the above variable relationships are relatively straightforward and may be found in most control system reference books (D'Azzo and Houpis, 1981). The net result is a chart of the form shown in Figure 4. The x- and y-axis variables are the open-loop phase and gain, respectively. The M-contours represent the gain of the closed-loop transfer function. The p-contours represent the corresponding phase angle of the closed-loop transfer function. By plotting the gain and phase of an arbitrary open-loop transfer function on such a chart, the result of closing the loop about the open-loop transfer function can be immediately determined by simply reading off M and p values for the closed-loop frequency response. This technique is closely related to the M-circle concept used for Nyquist diagrams.

Figure 4. Nichols Chart



The utility of such a graphical device is that the resonance/attenuation of the closed-loop system, implicitly revealed as the ratio of the two vectors, Y_0 and $1 + Y_0$, on a Nyquist diagram, is explicitly presented on a Nichols chart in the form of M-contours. Similarly, the closed-loop phase angle, represented on a Nyquist diagram as the phase angle difference between the Y_0 and $1 + Y_0$ vectors, is available directly from the p-contours on a Nichols chart. When typical driver/vehicle open-loop frequency response characteristics (as measured from experimental tests) are plotted on a Nichols chart, far more information concerning the closed-loop system response is available than if displayed in a Bode plot form.

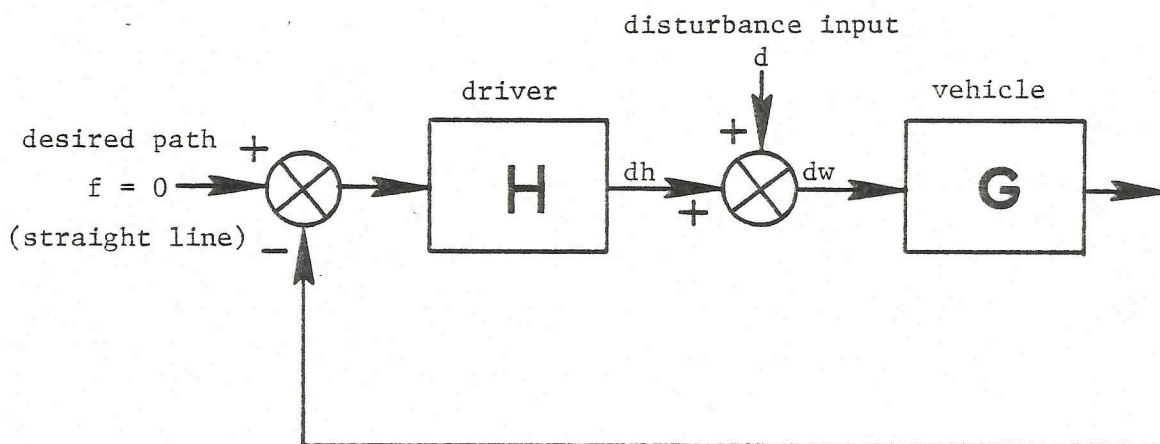
The next few sections serve to illustrate and compare each of these same methods for frequency response data obtained from both driver/vehicle experimental measurements and a mathematical model of the driver/vehicle system.

EXPERIMENTAL MEASUREMENTS OF DRIVER/VEHICLE FREQUENCY RESPONSE

Relatively few frequency response measurements of driver/vehicle directional control appear in the literature. The work of McRuer and Weir (McRuer, et al., 1975(b); Weir, et al., 1977) stands nearly alone in this particular area, only by virtue of so few other examples. Before presenting such measurements, the nature of the experimental driver/vehicle tests from which such measurements are derived will first be explained. It should be noted that the goal of such tests is to experimentally identify the combined driver/vehicle describing (transfer) function during straight-line regulatory driving.

Reference to Figure 5 shows a block diagram of a driver/vehicle closed-loop system with a disturbance input, d , applied at a summing

Figure 5. Disturbance Test Block Diagram



junction located at the output of the driver steering control block, H. The task for the driver during such a test is to provide a compensating steering control, dh , so as to offset the disturbance input, thereby maintaining the vehicle along a straight-line path. The sum of the driver's steering control, dh , and disturbance, d , form the front-wheel angle, dw , applied to the vehicle. The error signal between the driver steering response and the known external disturbance represents the input variable to the combined driver/vehicle (open-loop) system. The driver steering response constitutes the output variable. It can be shown (McRuer, et al., 1975(b)) that the combined driver/vehicle, open-loop transfer function (ignoring any driver remnant noise) is given by the Fourier transform of the quantity:

$$d/dw - 1 \quad (3)$$

Since the disturbance input, d , is known (e.g., a random appearing sum of several sinusoids, or low-pass, filtered white noise) and dh or dw is measured, the $(d/dw - 1)$ time history quantity is readily determined. By calculating the Fourier transform of the above-measured time history, the frequency response (gain and phase) of the combined driver/vehicle (HG), open-loop transfer function can be identified. A servomechanism controller which accepts the sum of the programmed disturbance signal and the driver steering output is typically used to generate the front-wheel steer angle, dw , in such a test arrangement.

Figure 6 shows a typical set of experimental measurements presented in a Bode plot form for four different vehicles labeled A, B, C, and D, and a single group of sixteen drivers (Weir, et al., 1977). Each of the four plots corresponds to one vehicle and the average group response of the sixteen drivers. The data were collected by means of the same test procedure described above during straight-line driving using an applied steering disturbance of five sinusoids. The four vehicles differed only in the level of understeer (2-7 degrees/g) and steering gear ratio (9:1 - 25:1). Each of these vehicle characteristics were achieved through use of a special, variable steering servo apparatus that permitted control and definition of the vehicle directional dynamics and steering ratio (McRuer, et al., 1975(a)). Table 1 summarizes the four vehicle configurations.

Table 1. Summary of Vehicle Characteristics

<u>Vehicle</u>	<u>Understeer (K)</u>	<u>Steering Gear Ratio</u>
A	2.4 deg/g	25:1
B	2.5 deg/g	17:1
C	5.6 deg/g	9:1
D	6.8 deg/g	11:1

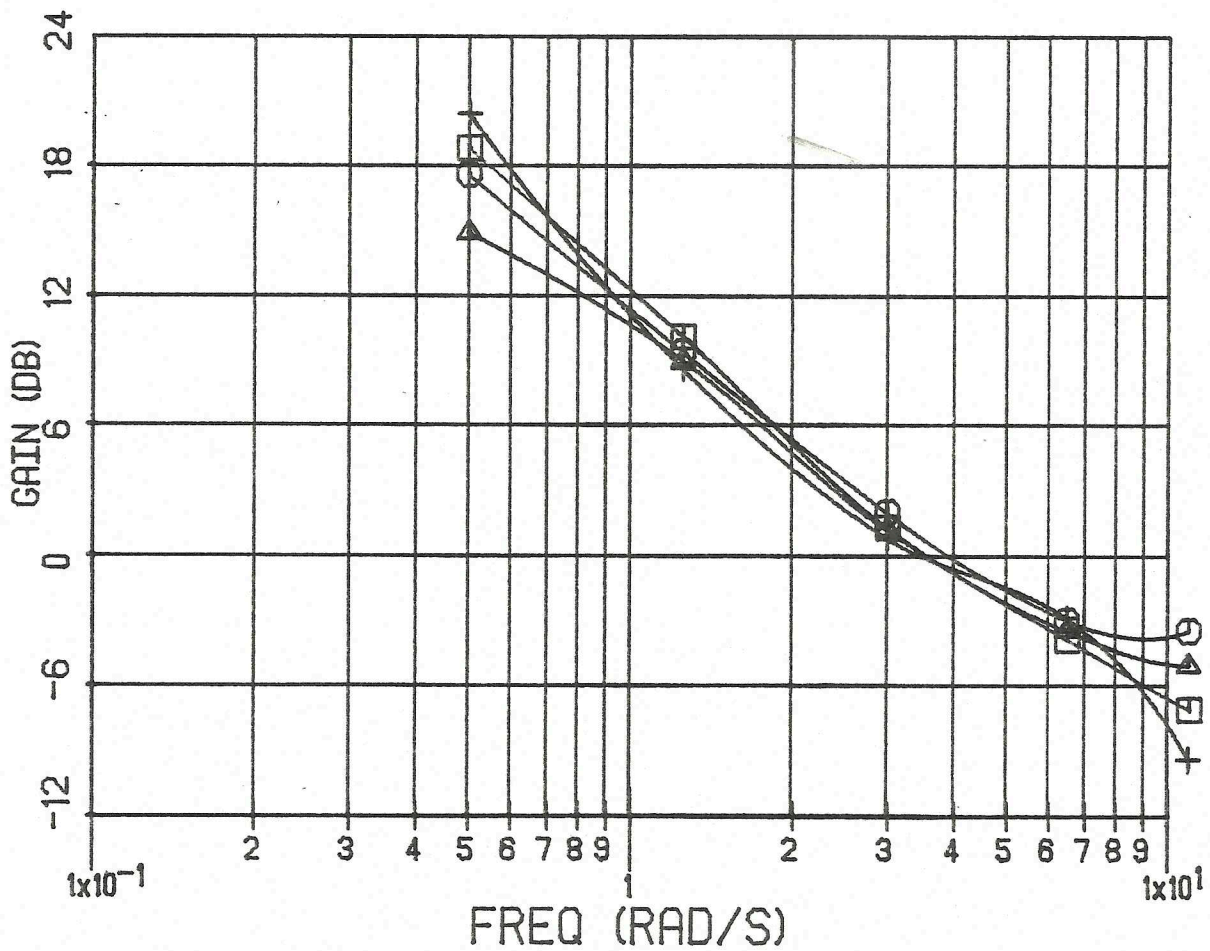
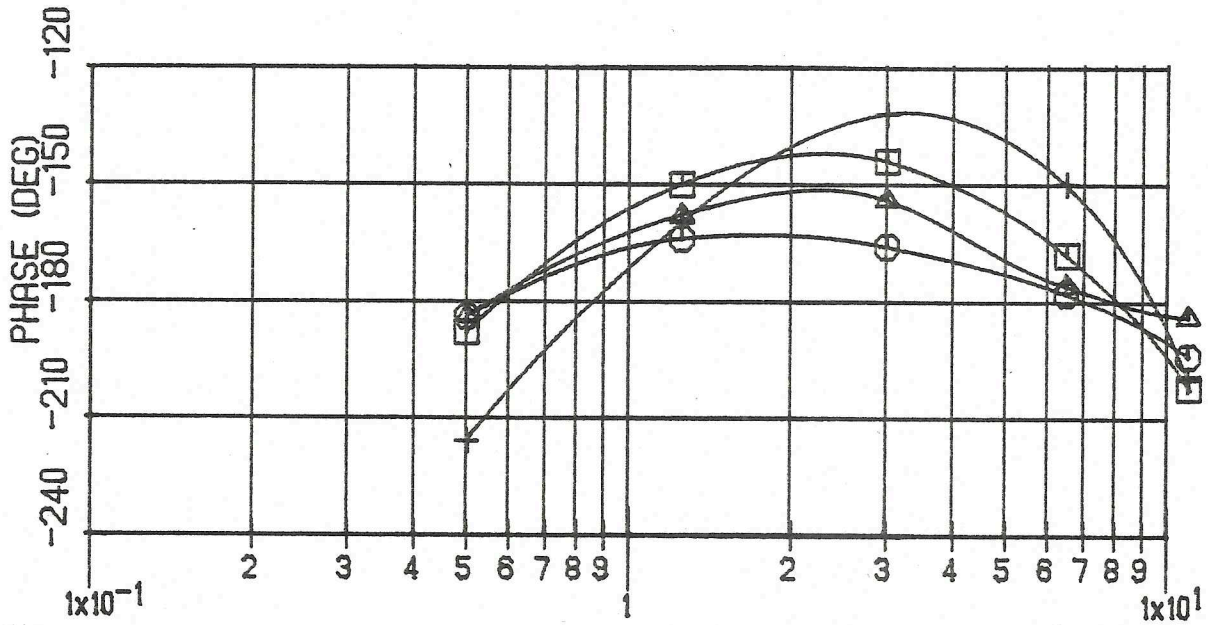
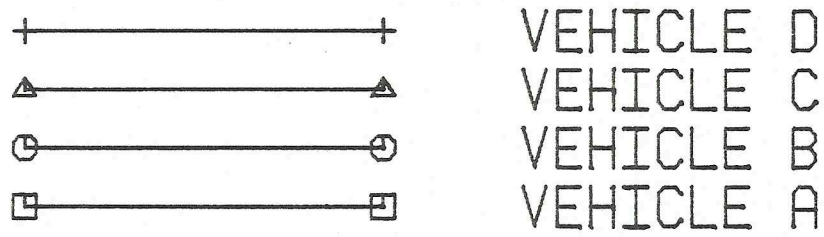
Weight of all vehicles: 2013 kg (4440 lb)

Wheelbase of all vehicles: 2.79 m (110 inches)

Test speed: 22.4 m/s (50 mph)

The experimental measurements of the open-loop, driver/vehicle transfer function (HG) appearing in Figure 6 display an approximate -6 db/octave slope for the gain characteristic with crossover frequencies ranging between 3.5 to 4.0 radians/second. The phase angle measurements display the familiar "peaking" characteristic observed very often in data of this kind within the frequency range of 1 to 4 radians/second.

Figure 6. Bode Plot of Driver/Vehicle Experimental Measurements



The relative vehicle rankings of closed-loop system stability based on the phase margin "rule of thumb" is seen to be: D,A,C,B -- D being the most stable. The least stable driver/vehicle system is B, having a phase margin of about 10 degrees.

Figure 7 shows these same data displayed (using two different scales) on a Nyquist diagram. Recalling that the critical point is located at (1,180 degrees) on this plot, the driver/vehicle systems are ranked in the same order as suggested by the Bode plot. That is, vehicle D exhibits a peak resonance ($|Y_o|/|1 + Y_o|$) in the vicinity of crossover (unity magnitude) equal to about 1.3, while vehicle B has a corresponding value of about 5.0 in the same frequency range. Hence we see that for these data, the phase margin "rule of thumb" associated with the Bode plot provides a good measure of the relative stability of the closed-loop systems when verified and checked against the more complete analysis offered by the Nyquist diagram. The Nyquist analysis confirms that the actual peak resonance values for each of these data sets, though not occurring at crossover, do occur at frequencies in the vicinity of crossover.

Lastly, Figure 8 shows these same experimental data presented on a Nichols chart. It now becomes very clear what the maximum resonance value (stability measure) is for each driver/vehicle combination and in what frequency range it occurs. For example, B, C, and A each reach maximum resonances (largest M-contour values) just above crossover (negative db values for $|Y_o|$). The maximum resonance values read from this chart are approximately 14 db (5.0), 10 db (3.2), and 6 db (2.0), respectively. Driver/vehicle combination D, the most stable configuration, reaches its maximum resonance significantly below crossover (positive db values for $|Y_o|$) with a value of about 4 db (1.6). At very low frequencies all the vehicle combinations will approach the 0 db M-contour corresponding to large, open-loop gain values and -270 degrees of phase shift.

The Nichols chart of Figure 8 also illustrates, very directly, the influence upon the closed-loop system response of changing the gain or phase of the open-loop transfer function. For example, an increased open-loop gain corresponds simply to an upward shift of the frequency response locus, and a constant increase in phase angle to a rightward shift of the locus. Thus, by way of example, if driver/vehicle configuration B was able to lower its open-loop gain by approximately -6 db (0.50), a significant improvement in closed-loop stability would result, with the maximum resonance dropping from 14 db to about 11 db. A similar result would be obtained for any reduction in open-loop transfer function time lags productive of about a 5-10 degree increase in phase angle at the upper frequencies (e.g., a 0.03 second decrease in an open-loop transport lag).

DRIVER/VEHICLE FREQUENCY RESPONSE CORRESPONDING TO MORE EXTREME VARIATIONS IN VEHICLE AND DRIVER PROPERTIES AS PREDICTED BY A MATHEMATICAL MODEL

In order to examine the influence of more dramatic variations in vehicle properties and driver properties upon the nature and appearance of each of the discussed plots, a mathematical model of the driver/vehicle system (MacAdam, 1981) is employed in this section to calculate frequency response characteristics. The vehicle component of the driver/vehicle model is essentially a linear, two-degree-of-freedom (lateral and yaw motions) representation, including lateral path displacement and heading angle. The driver component is a preview control which synthesizes closed-loop steering control based on vehicle dynamics

Figure 7. Nyquist Diagram of Driver/Vehicle Experimental Measurements

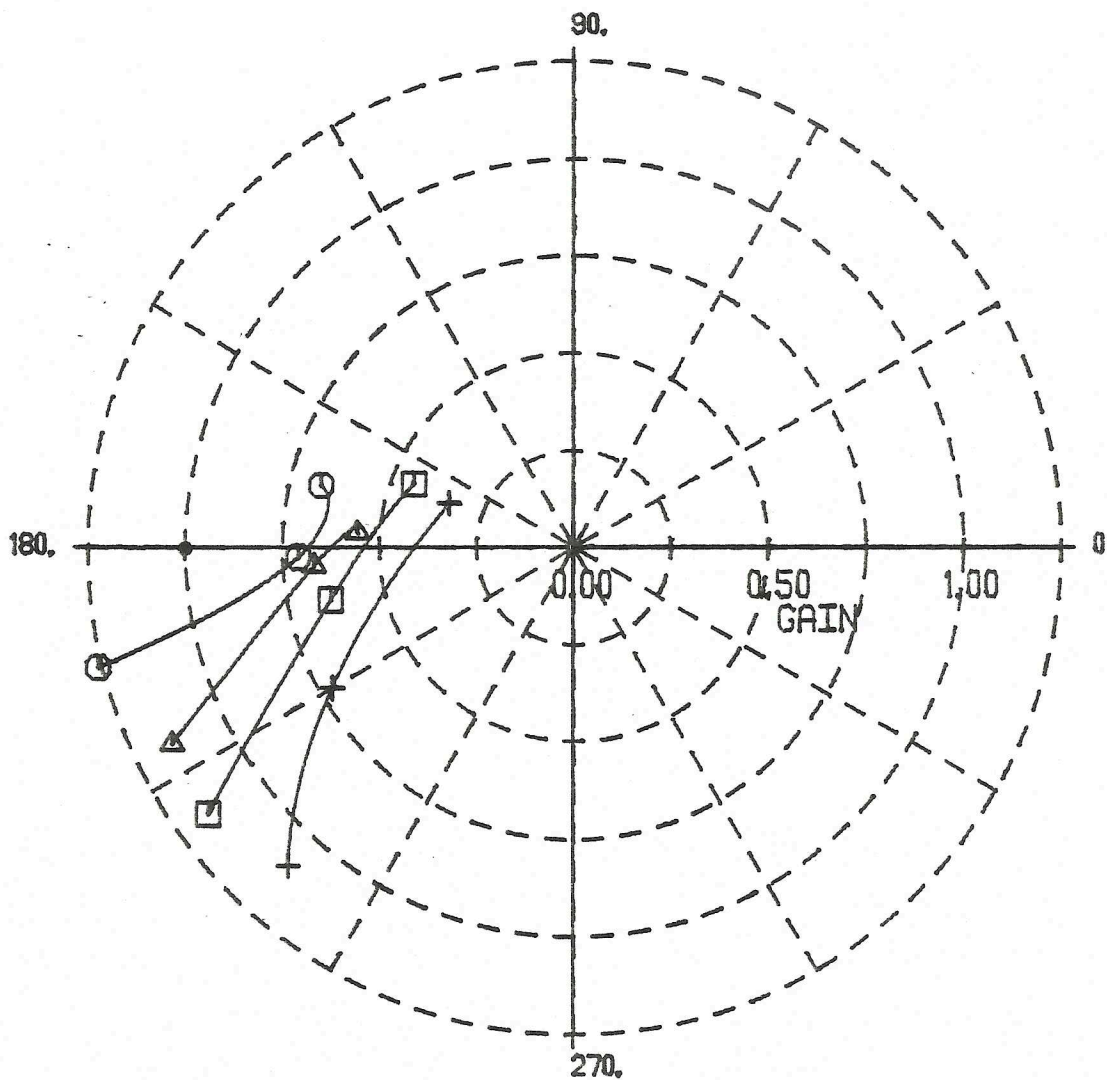
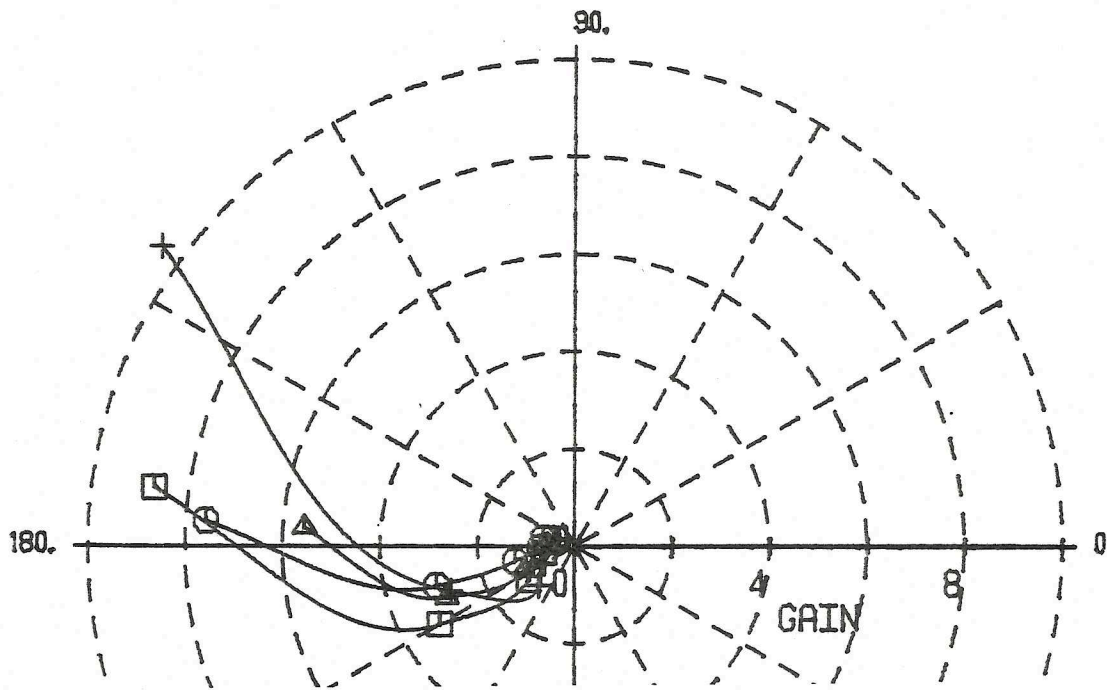
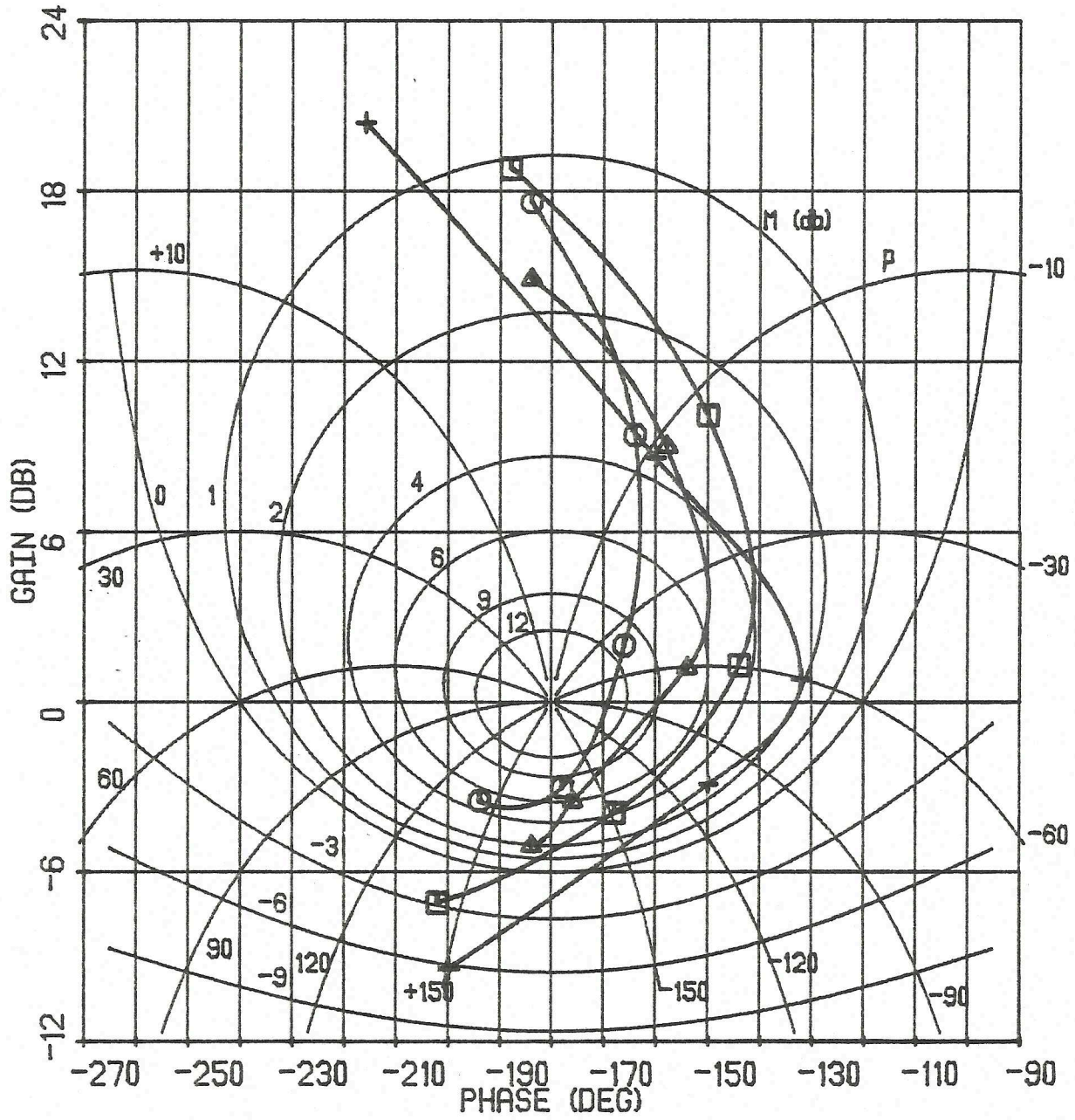


Figure 8. Nichols Chart of Driver/Vehicle Experimental Measurements



information defined by the vehicle properties, a specified driver preview time, and a specified driver transport lag.

Variations in Vehicle Properties

Figure 9 shows 22.4 m/s (50 mph) frequency response calculations predicted by the driver/vehicle model for three variations in vehicle understeer (7, 0, and -7 degrees/g). These calculations are equivalent to the frequency response measurements of the driver/vehicle, open-loop, describing function presented in the previous section. The vehicle dynamic properties for the 7 degree/g vehicle are defined by the parameter list contained in Appendix A of (MacAdam, 1981), and corresponds closely to vehicle D of the previous section. The driver model preview time and transport lag parameters are held fixed at values of 2.25 seconds and 0.28 seconds for the calculations shown in Figure 9. The transition from understeer (7 deg/g) to neutral steer (0 deg/g) to oversteer (-7 deg/g) was achieved by reducing the cornering stiffness of the rear tires. The extreme -7 deg/g oversteer vehicle is directionally unstable (open-loop) at this speed, operating above its critical velocity of 15.2 m/s (34 mph). However, the closed-loop (driver-controlled) system is stable, but only marginally so. Reference to Figure 9 and invocation of the phase margin "rule of thumb" would not indicate a marginally stable driver/vehicle system but rather, a highly stable, well-damped system. Use of the phase margin rule in this case leads to confusion since three separate crossover frequencies are indicated, two implying instability, the other implying a very stable system. How such an assessment of closed-loop system stability is accurately determined is presented in Figure 10.

Figure 10 shows a Nyquist diagram for the same data seen in the Bode plot of Figure 9. The locus corresponding to the -7 deg/g vehicle is distinctly different from the two remaining loci by wrapping itself about the origin more tightly, and in doing so, coming very close to the (1,180 degree) critical point at a frequency of about 1.5 radians/second. The maximum closed-loop resonance, $|Y_o|/|1 + Y_o|$ near the critical point is about 6. At lower frequencies, the Nyquist diagram for the open-loop oversteer vehicle continues to decrease in phase angle, eventually approaching -450 degrees with very large values of gain. Because a sign reversal occurs in the open-loop directional dynamics of the oversteer vehicle when operating above its critical velocity, such driver/vehicle data will display an additional 180 degrees of negative phase shift over driver/vehicle systems which contain directionally stable vehicle dynamics. The 7 deg/g and 0 deg/g vehicles, which are open-loop directionally stable, will approach the more conventional -270 degree phase shift condition at very low frequencies.

The principal difference noted here in closed-loop system stability for the 7 deg/g and 0 deg/g vehicles is a slight advantage for the understeer vehicle. However, this result applies only for a fixed set of driver characteristics (2.25-second preview, 0.28-second transport lag). Without examining other driver parameter combinations and determining whether or not different vehicle dynamic characteristics promote different driver preview preferences, conclusions concerning "optimal" levels of vehicle understeer or related questions cannot be objectively offered.

Finally, Figure 11 shows these same frequency response characteristics plotted on a Nichols chart. The most noteworthy item here is the behavior, again, of the unstable (open-loop), oversteer vehicle, causing the locus to wrap sharply around the Nichols chart origin. It is seen from this chart that the maximum closed-loop system resonance of 16 db (6.0) occurs at an open-loop gain of about 1.5 db and -180

Figure 9. Mathematical Model Predictions of Driver/Vehicle Response
 Due To Vehicle Understeer, K, Variations; Bode Plot.

\triangle ————— \triangle $K = -7 \text{ DEG/G}$
 \circ ————— \circ $K = 0 \text{ DEG/G}$
 \square ————— \square $K = 7 \text{ DEG/G}$

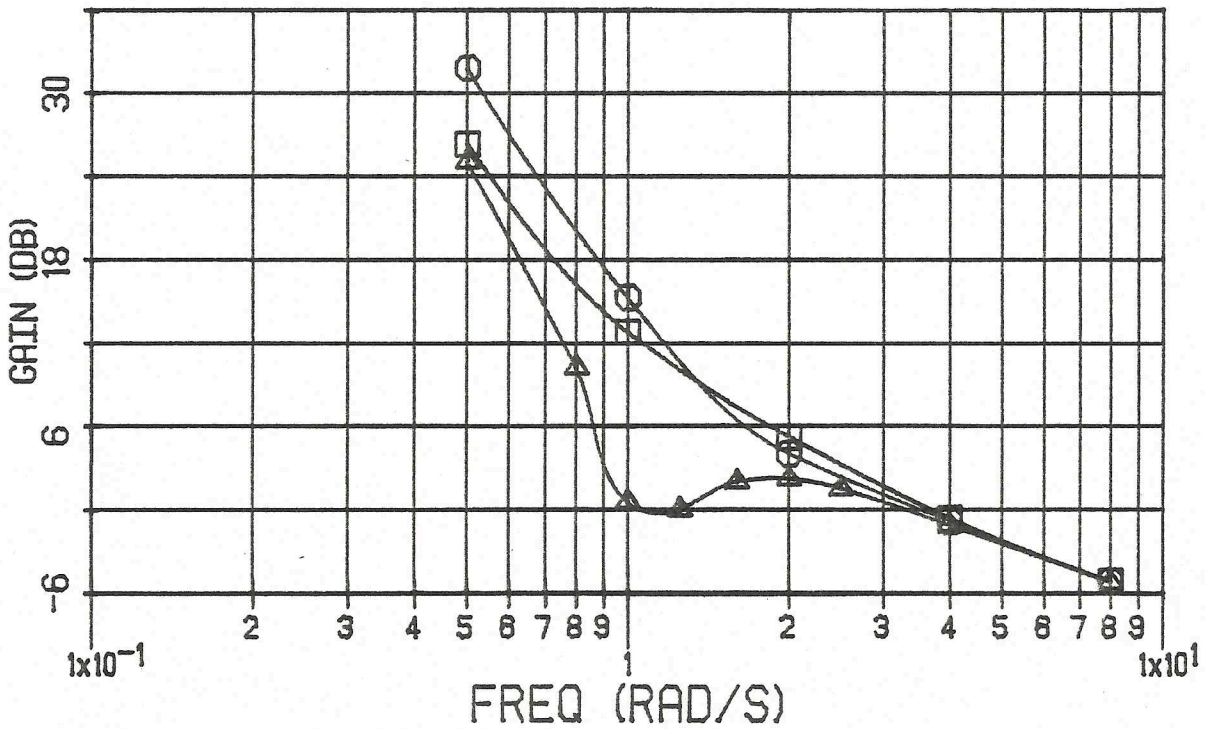
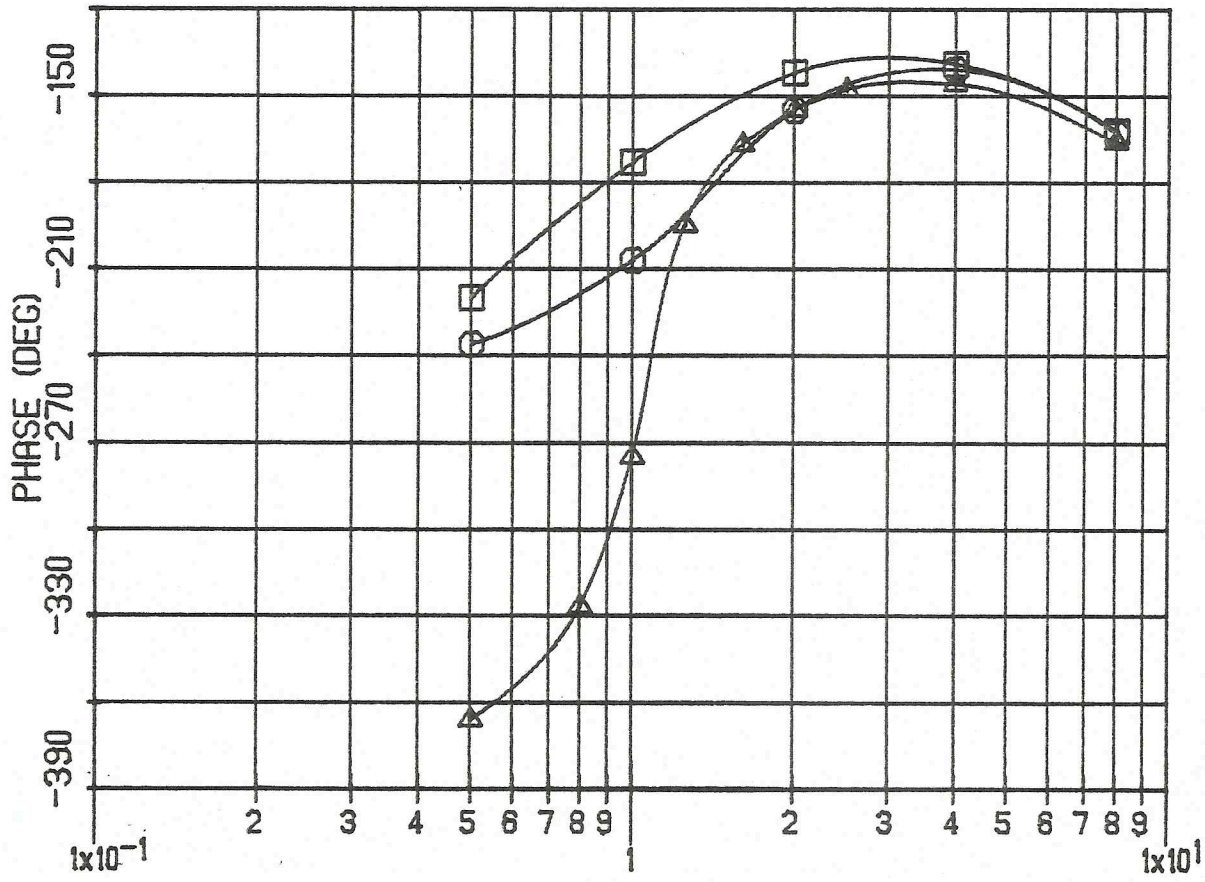


Figure 10. Mathematical Model Predictions of Driver/Vehicle Response
Due To Vehicle Understeer, K, Variations; Nyquist Diagram.

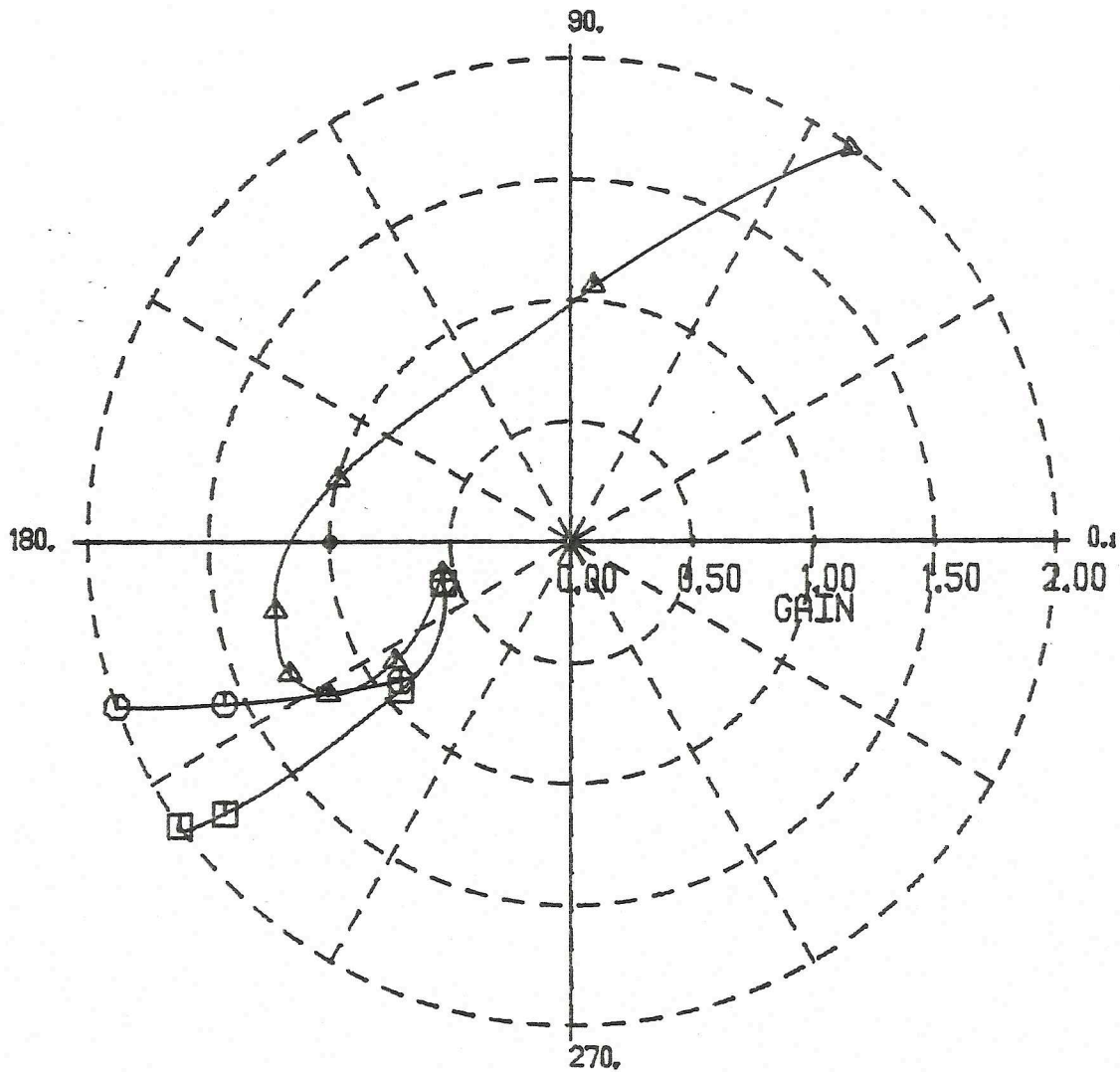
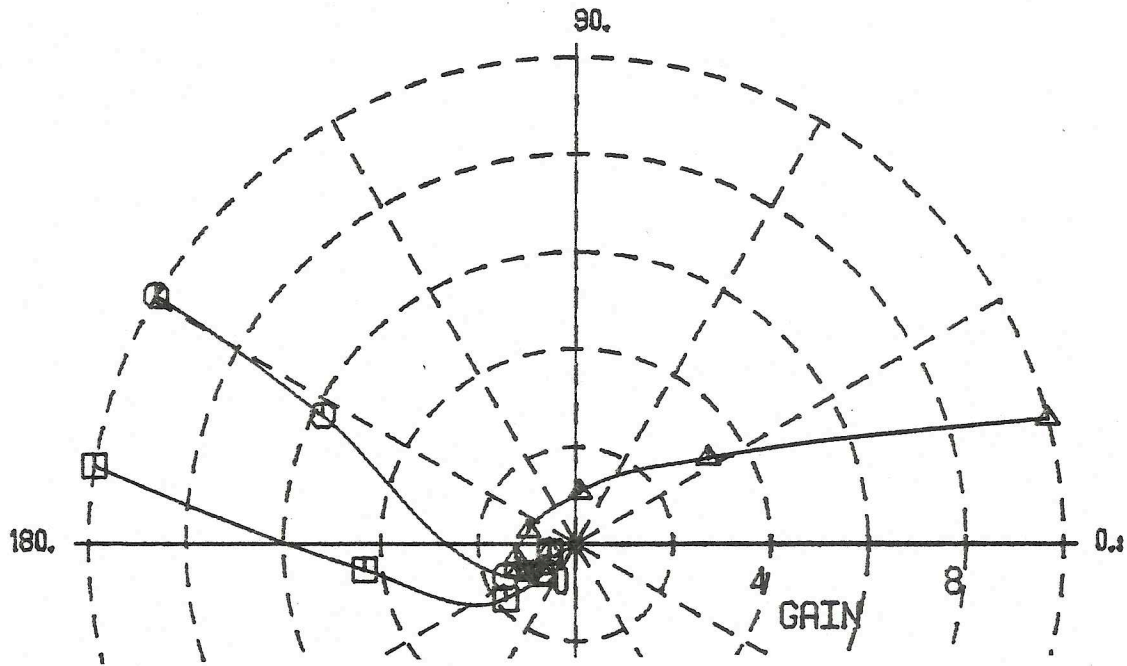
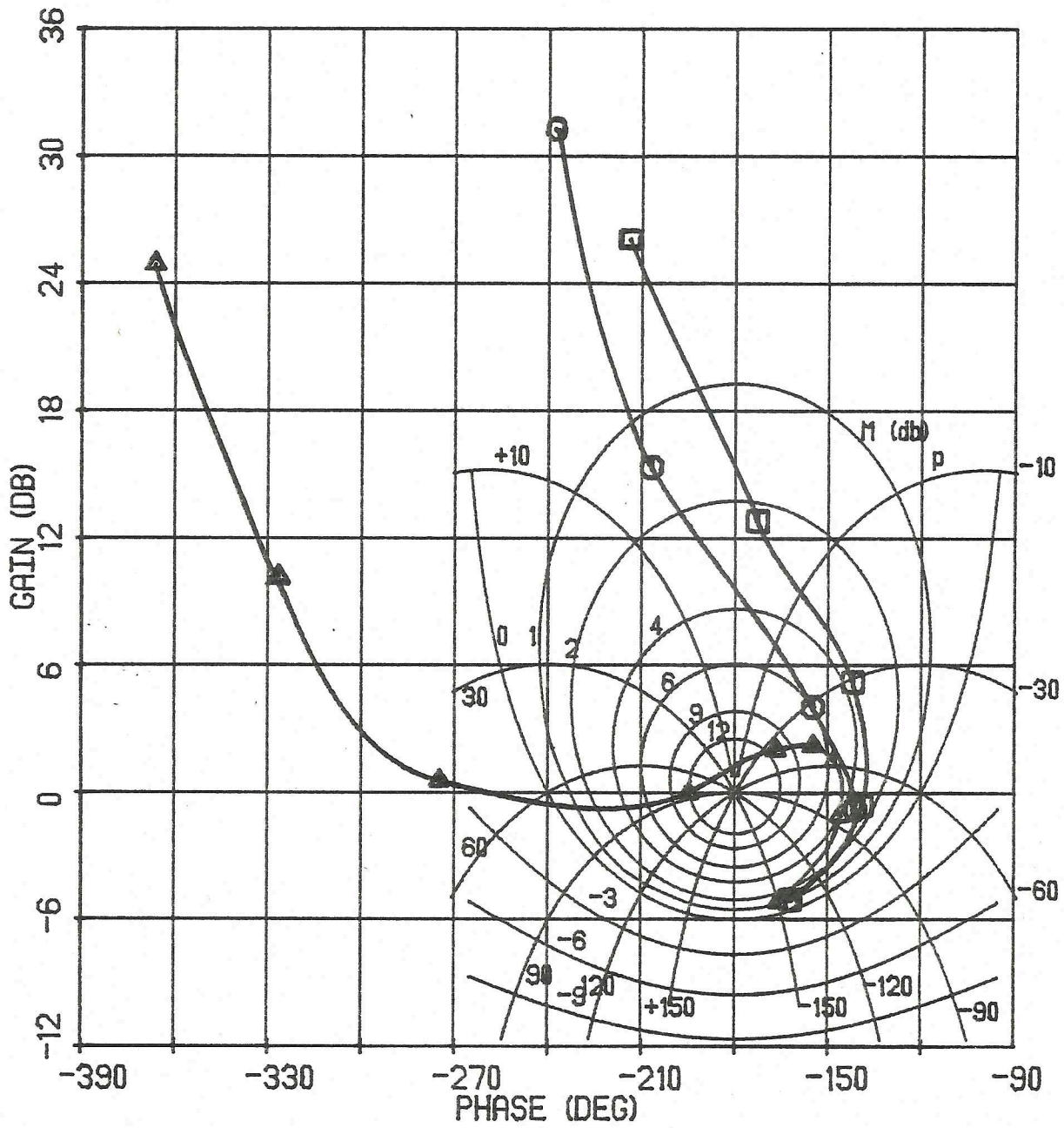


Figure 11. Mathematical Model Predictions of Driver/Vehicle Response Due To Vehicle Understeer, K , Variations; Nichols Chart.



degrees phase shift (approximately 1.5 radians/second). The understeer vehicle exhibits a maximum closed-loop resonance of approximately 3.5 db (1.5) while the neutral steer vehicle has a maximum resonance of 6 db (2.0), each in the vicinity of 2 radians/second.

Variations in Driver Control Characteristics

Variations in driver control characteristics, as represented by the preview time ("look ahead" time used by the driver) driver model parameter (TP), are shown in the Bode plot of Figure 12. The 7 deg/g understeer vehicle dynamics of the preceding discussion were used here for all preview parameter variations. As seen, the variations in preview available to drivers is a particularly powerful means of modifying and defining the open-loop driver/vehicle frequency response characteristics. Figure 13 displays these same data on a Nyquist diagram. The decrease in system stability accompanying decreased preview times is intuitively understood and analogous to restricting a driver's view of the roadway. Routine circumstances occurring in everyday driving which require drivers to alter their preview times in the interest of maneuverability (e.g., different path-following requirements or obstacle-avoidance maneuvers) might therefore imply a compromise between closed-loop system stability and maneuverability. This issue is discussed somewhat further in the final section of the paper.

Lastly, presentation of the driver preview time variations on a Nichols chart is seen in Figure 14. The 1.0-second preview case shows a maximum closed-loop resonance of 16 db (6.0) occurring just above crossover at an open-loop gain of about 1 db and -175 degrees phase shift. In contrast, the 3.5-second preview case shows a maximum closed-loop resonance of less than 0.25 db (1.03) occurring for an open-loop gain of approximately 12 db and -105 degrees phase shift (frequency of 1 radian/second). The results presented in Figure 14 underscore, again, the strength of the preview control mechanism available to drivers in largely determining the directional stability of the closed-loop system.

MANEUVERABILITY OF DRIVER/VEHICLE SYSTEMS

The material presented in previous sections has been primarily concerned with matters of relative stability of driver/vehicle systems and associated methods of analysis. The material which follows attempts to examine the topic of driver/vehicle maneuverability and its relationship to the earlier topic of closed-loop system stability. The term "maneuverability" is used here to describe the steady-state, path-tracking ability of a driver/vehicle system in response to a sinusoidal path input. For example, envision a test in which a driver is asked to follow a sinusoidal path laid out along a test course. If the forward velocity of the vehicle remains constant, the ability of the driver/vehicle system to accurately track this path will depend upon the spatial frequency of the path and the characteristics of the dynamic system. At low spatial frequencies the trajectory of the vehicle center of gravity will closely match the sinusoidal path. As the frequency of the path increases, the ability of the driver/vehicle system to replicate the path will become degraded. At high enough frequencies, the system will not be capable of responding and will simply move in a straight line down the center of the course. At intermediate frequencies, the system path response will become attenuated, or, in some cases, will resonate at certain frequencies prior to attenuating at higher frequencies. Exactly how a driver/vehicle system does respond under such conditions depends largely upon the driver control strategies and limitations (e.g., amount of preview used by the driver/driver lags).

Figure 12. Mathematical Model Predictions of Driver/Vehicle Response
 Due To Driver Preview, TP, Variations; Bode Plot.

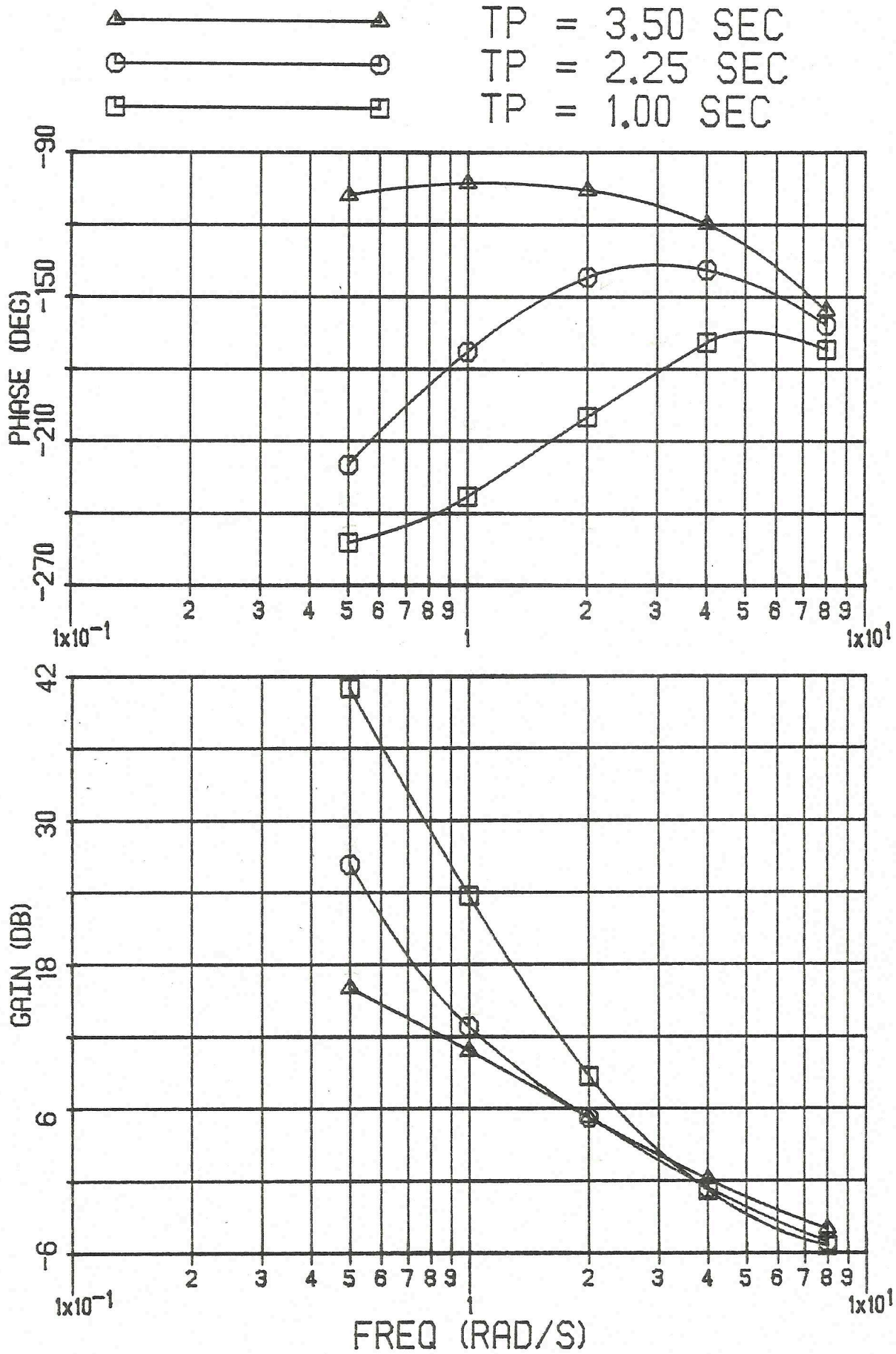


Figure 13. Mathematical Model Predictions of Driver/Vehicle Response
Due To Driver Preview, TP, Variations; Nyquist Diagram.

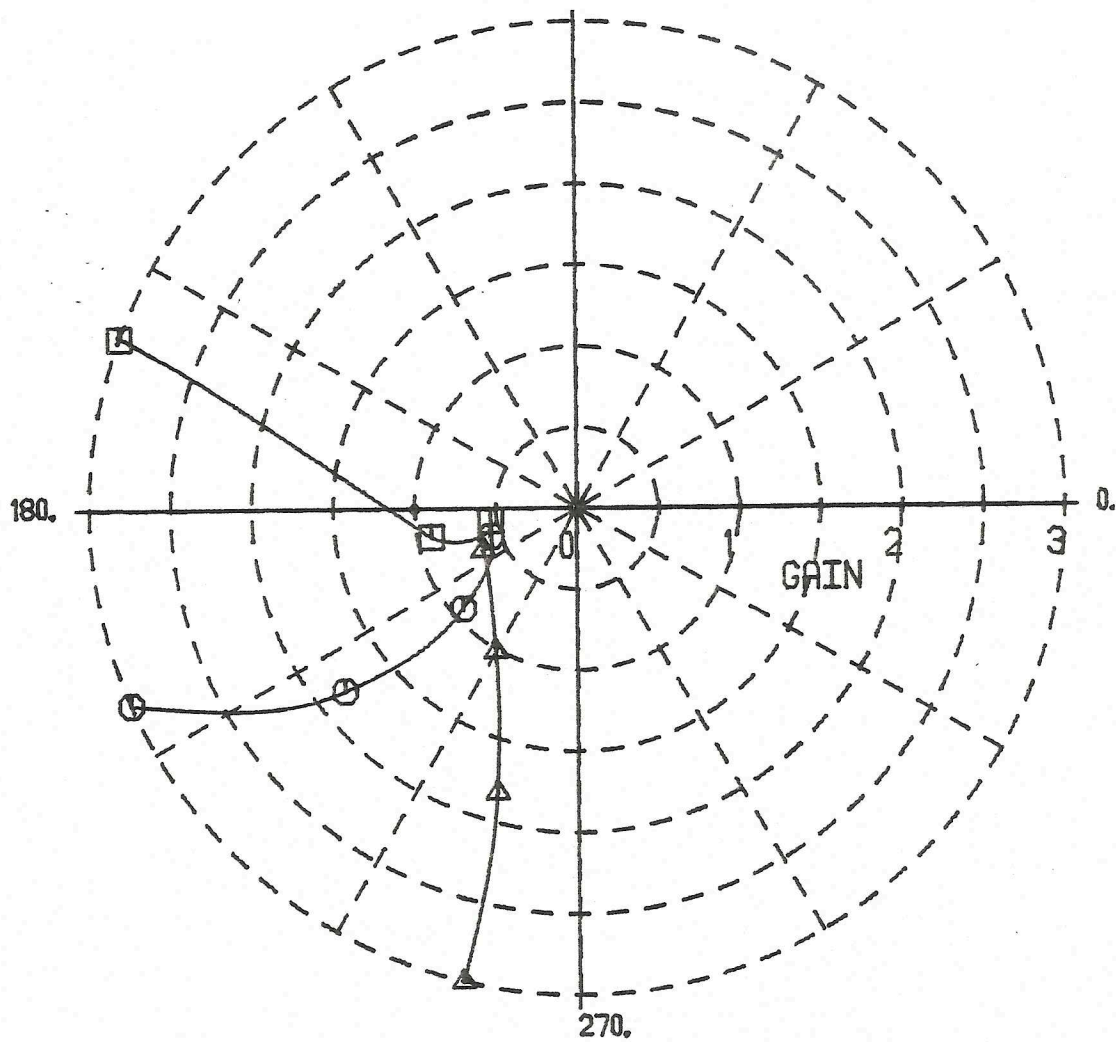
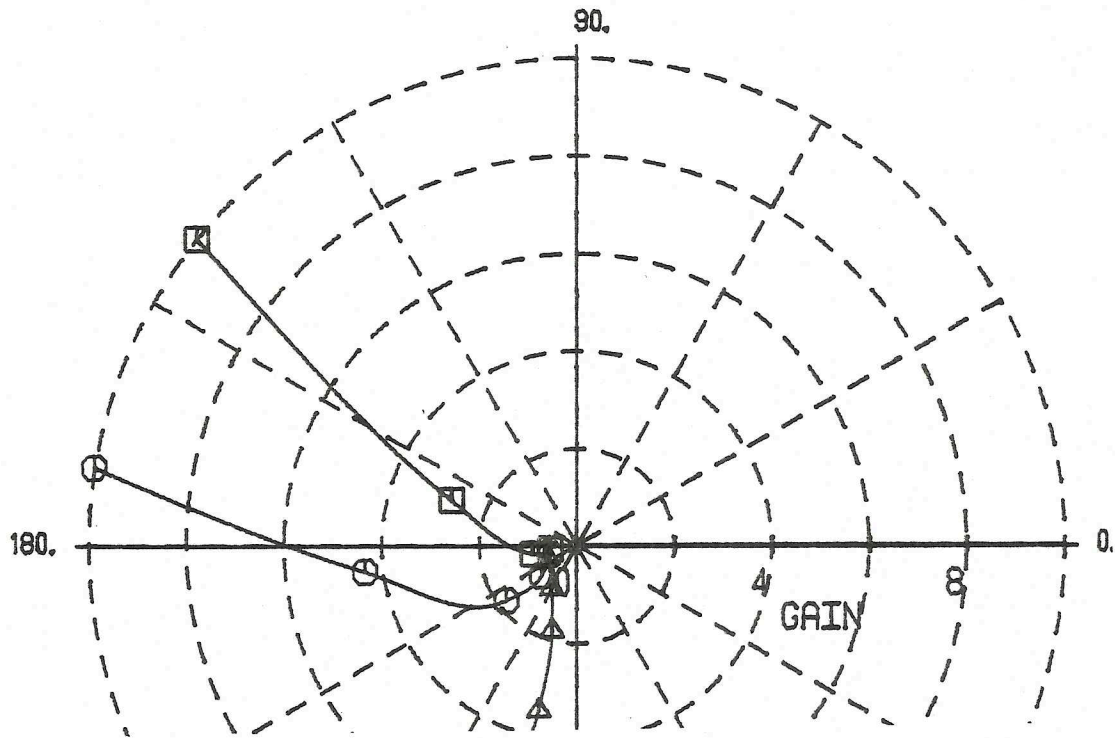
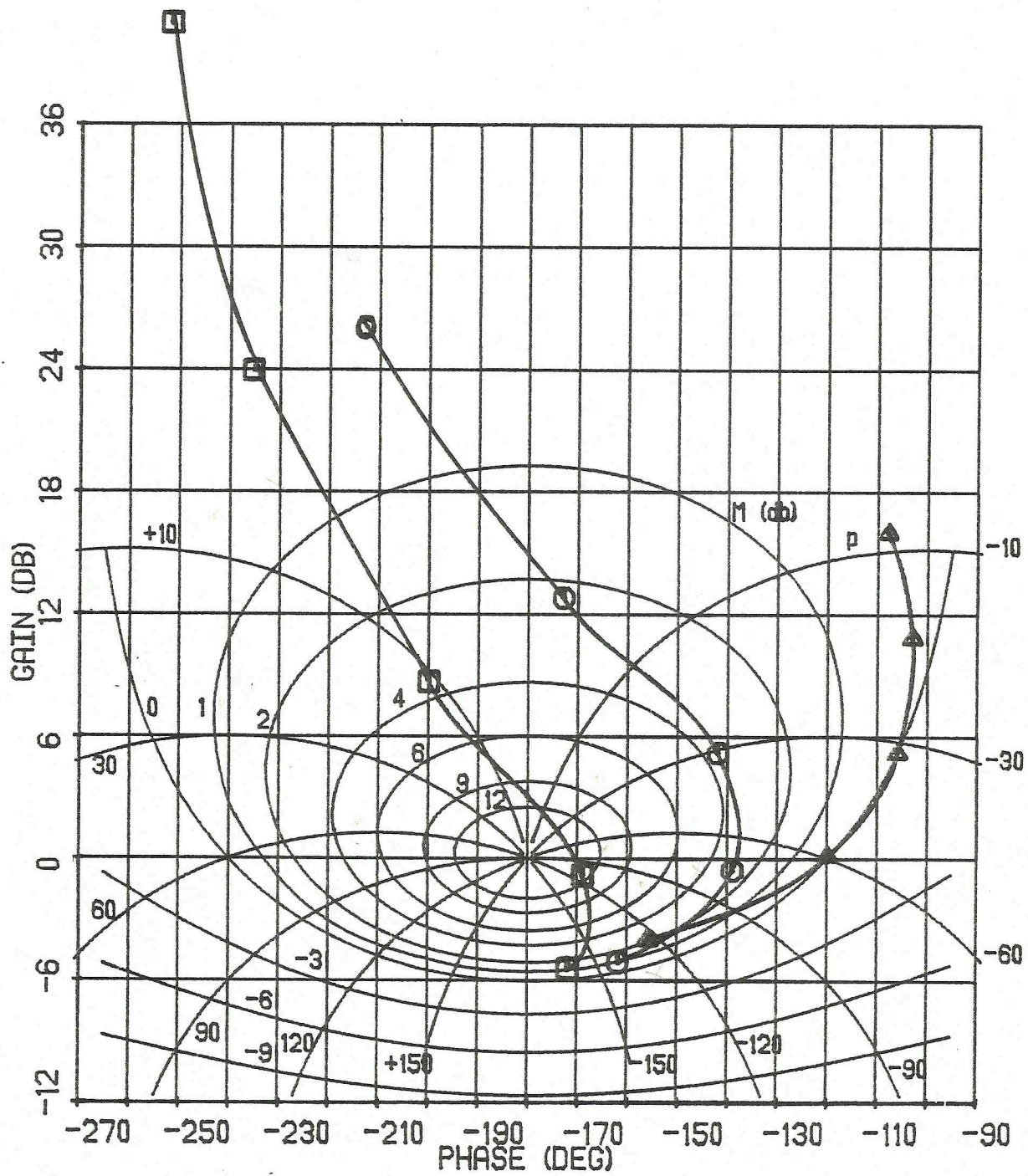


Figure 14. Mathematical Model Predictions of Driver/Vehicle Response Due To Driver Preview, TP, Variations; Nichols Chart.



One way of describing this path-tracking ability, or closed-loop maneuverability, of the driver/vehicle system is to consider a frequency response function, $F(jw)$, relating the vehicle center of gravity lateral displacement, y , to the lateral displacement of the path input, y_p , for various path input frequencies, w :

$$y/y_p = F(jw) \quad (4)$$

For low sinusoidal input frequencies of y_p we would expect $F(jw)$ to have a gain of unity and zero phase angle. As frequency increases, $F(jw)$ would eventually attenuate, possibly displaying some resonance at intermediate frequencies. Increased phase lag would accompany the higher frequencies as well.

Precisely this approach was adopted in this section in order to examine the maneuverability of closed-loop driver/vehicle systems. The mathematical model of the driver/vehicle system (MacAdam, 1981) used in the previous section is employed here to calculate $F(jw)$. Note that the frequency response calculations/measurements and resonances discussed in the previous two sections in connection with closed-loop system stability are not the same calculations or resonances being discussed here. The former frequency response calculations associated with stability of the closed-loop system are analogous to the frequency response relating driver-estimated future vehicle position to previewed path errors—a quantity that depends largely upon the inner control loops synthesized by drivers attempting to follow a previewed path. This preview strategy, of course, depends upon feedback queues involving each of the vehicle motion variables. In contrast, the $F(jw)$ measure discussed in this section is simply a direct result of the above driver steering control strategy, manifesting itself, slightly later in time, as a vehicle path displacement approximating the desired input path.

Figure 15 shows an example calculation of $F(jw)$ relating y/y_p versus path input frequency. The result shown here corresponds to the 7 deg/g understeer vehicle of the previous section operating at 22.4 m/s (50 mph) with a fixed driver preview time equal to 2.25 seconds and transport lag of 0.28 seconds. We see that at very low path input frequencies, the gain is unity and the phase angle is near zero. As frequency increases, the gain attenuates, reaching -20 db (0.1) and -50 degrees of phase shift at 2 radians/second. We conclude from Figure 15 that, at a path input frequency of 2 radians/second, this particular driver/vehicle configuration would reproduce only 10 percent of the amplitude of a 3-second-period sinewave path and be delayed in time 0.4 seconds (-50 degrees). The driver, as modeled here, is assumed to weight path errors equally over the preview interval and thus acts as a preview filter. It should be expected, therefore, that as the sinusoidal path input period decreases to a value equal to the driver preview time, the gain of $F(jw)$ will approach zero. This implies that the bandwidth of $F(jw)$, or closed-loop maneuverability limit, can be altered directly by drivers, simply by employing variable amounts of preview. The bottom portion of Figure 15 shows an example time history calculation of vehicle path corresponding to a 1.0 radian/second sinusoidal path input (6.3-second period) and a 2.25-second driver preview time.

Figure 16 shows the same calculation as seen in Figure 15 except for a reduced value of driver preview time of 1.0 seconds. We see a similar attenuation in $F(jw)$ at increased frequencies, but not until about 5 radians/second, or, sinewave periods approaching 1.0 second. Also seen on this plot is an indication of amplification or resonance in the vicinity of 3.2 radians/second (2-second sinewave period). This latter result would suggest that the driver/vehicle combination utilizing a 1.0-second preview time would "track" a 2-second sinewave of

Figure 15. $F(j\omega)$, Closed-Loop Frequency Response of Path Displacement;
 Preview (TP) = 2.25 sec; Driver Lag (TAU) = 0.28 sec.

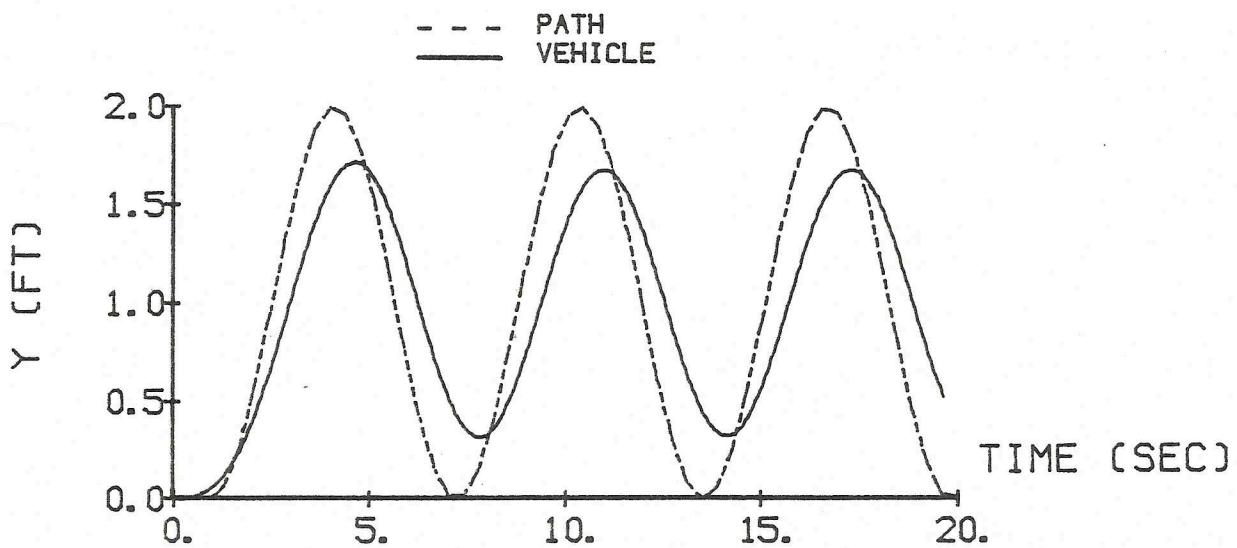
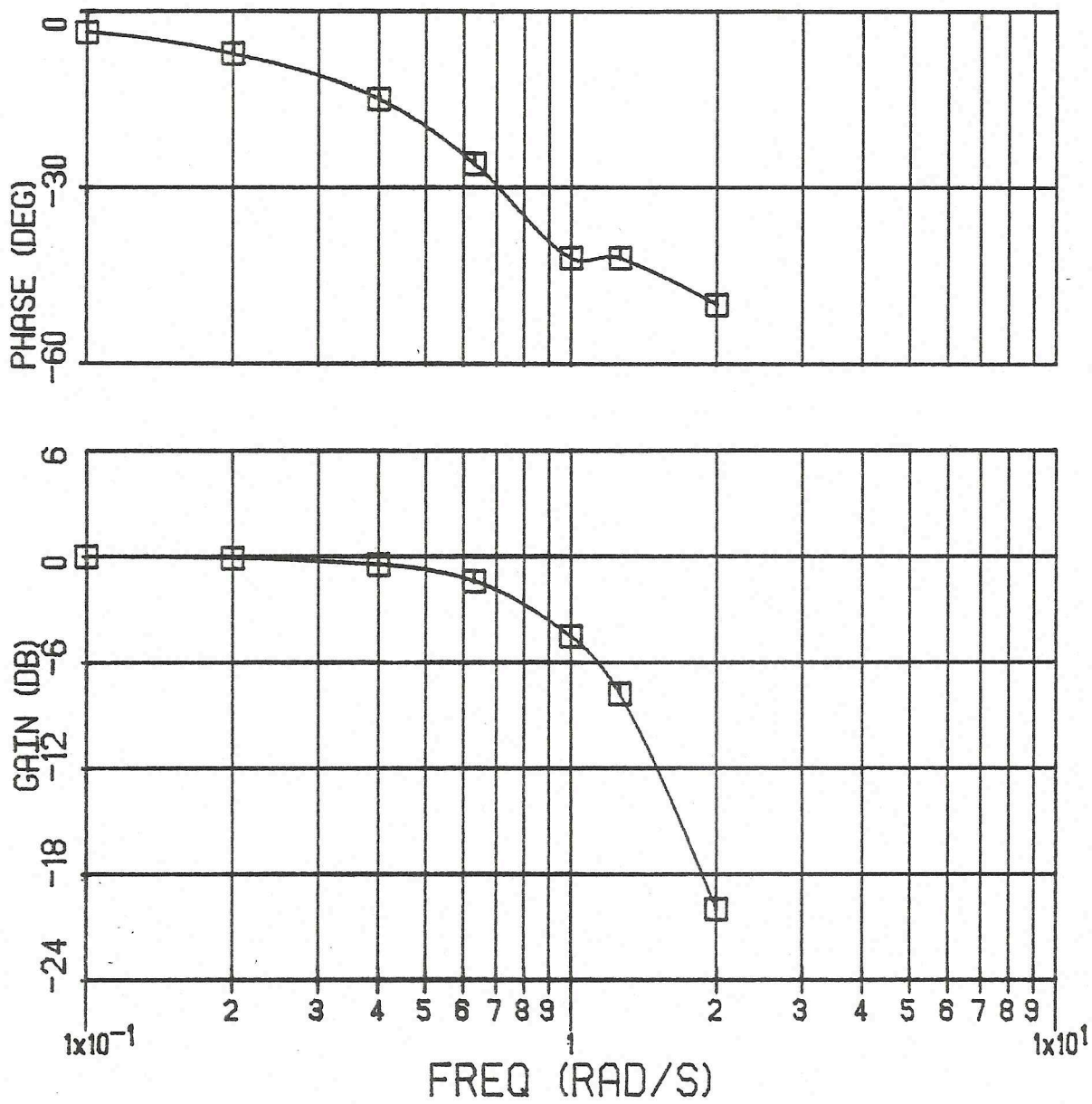
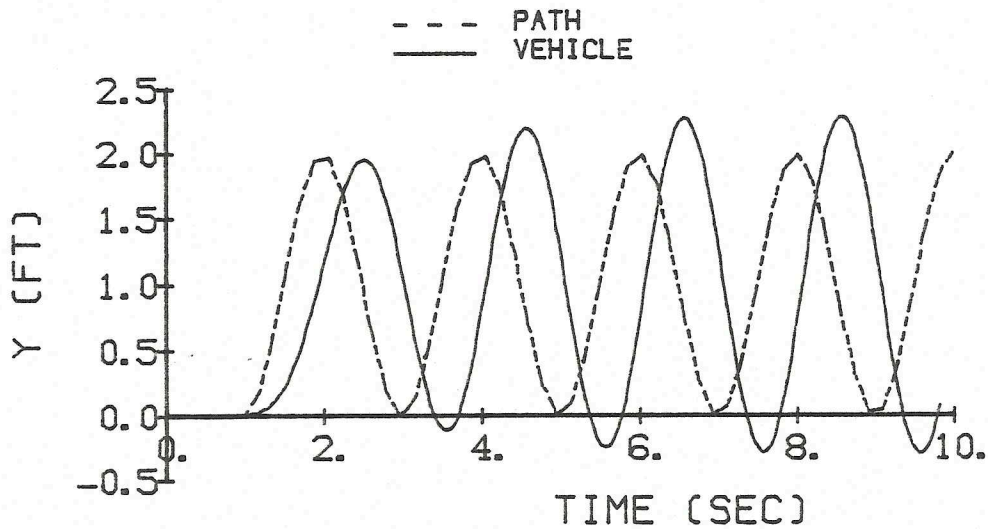
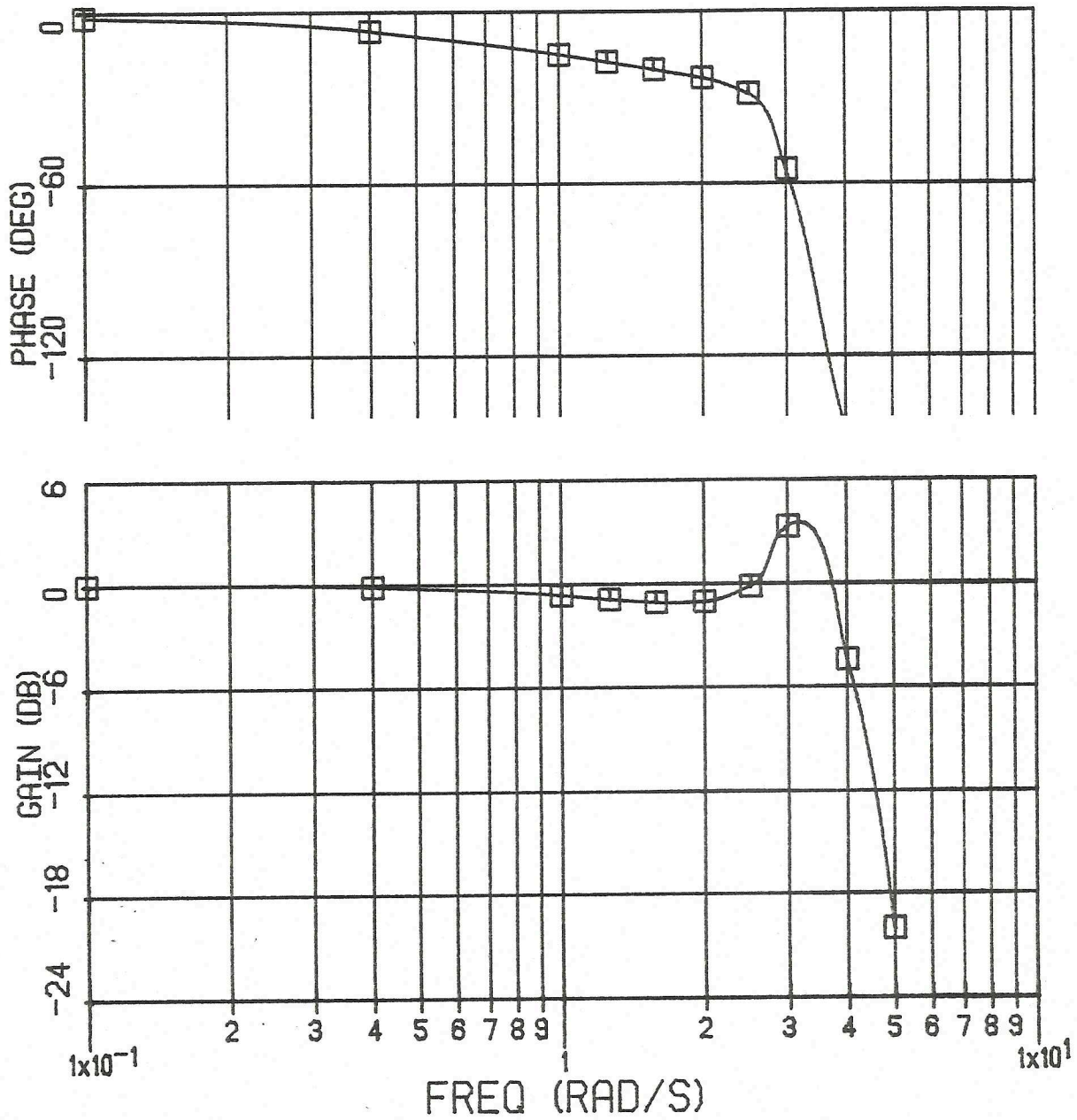


Figure 16. $F(j\omega)$, Closed-Loop Frequency Response of Path Displacement;
 Preview (TP) = 1.0 sec; Driver Lag (TAU) = 0.28 sec.



amplitude C with a sinusoidal vehicle path displacement of amplitude $1.4C$ while lagged in time 0.5 seconds (-90 degrees phase shift). A time history comparison of the vehicle lateral displacement and sinusoidal path is seen at the bottom of Figure 16, illustrating the path amplification observation.

The influence that driver transport lags can have on the appearance of $F(j\omega)$ is seen in Figure 17. The calculations appearing in Figures 15 and 16 are repeated here with driver transport lag values of 0.75 seconds and 0.28 seconds, respectively. In the first case corresponding to a driver preview time of 2.25 seconds, increasing the transport lag from 0.28 to 0.75 seconds precipitates path amplification in $F(j\omega)$. On the other hand, reducing the driver transport lag from 0.28 to 0.10 seconds in the 1.0-second preview case eliminates amplification in $F(j\omega)$. Although these driver transport lag variations are somewhat unrealistic, they do serve to illustrate the importance of the primary control response limitation inherent in human operators and its interplay with driver preview control strategy.

The net result deriving from the frequency response calculations of directional stability and those just presented for path maneuverability is the simple illustration that drivers, by altering their preview control strategies to satisfy different path-following requirements, may simultaneously trade off decreased closed-loop stability in exchange for increased path maneuverability. Thus, the transition by a driver from a 2.25-second preview time to a 1.0-second preview time for obtaining the increased path maneuverability suggested by Figures 15 and 16, will incur a "cost" of reduced system stability suggested in Figures 13 or 14.

The matter of tradeoff or compromise between closed-loop system stability and path maneuverability is a continual part of the normal driving process and which has not been, to date, adequately investigated by driver/vehicle testing. It would seem that sinusoidal path tests of the type suggested here, in combination with the disturbance tests outlined in the previous section, would provide the kind of pertinent information necessary for investigating this issue further from an experimental foothold. Furthermore, the type of driver/vehicle tests suggested are relatively simple to implement, easily conducted, and would be directly applicable to the frequency domain techniques and analyses examined above.

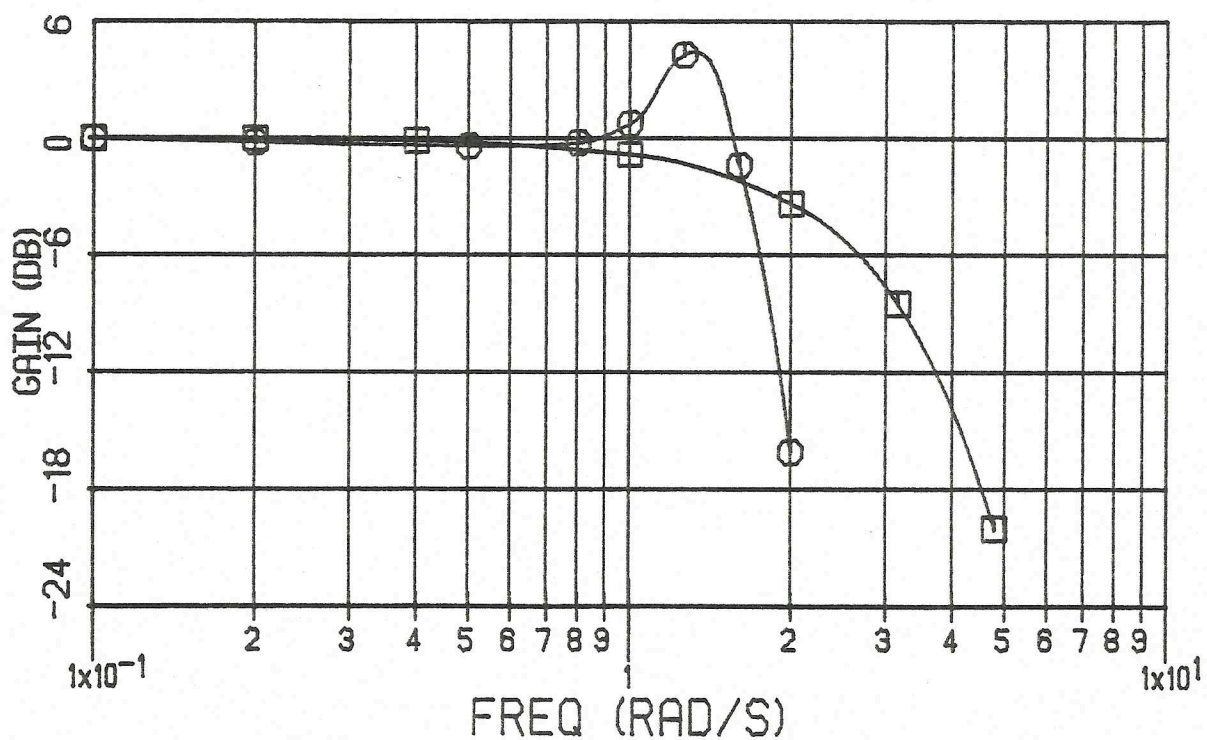
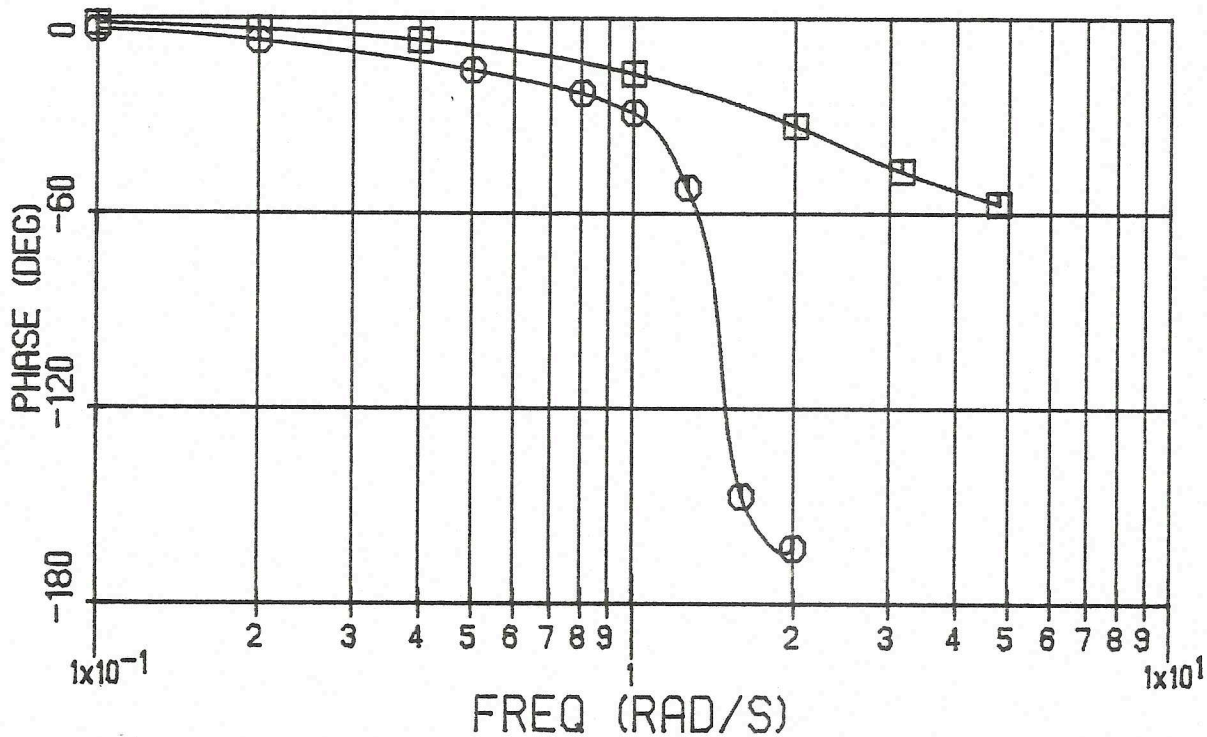
SUMMARY AND CONCLUSIONS

Several frequency domain techniques, useful for analyzing both experimental measurements and mathematical model predictions of driver/vehicle steering response, have been presented and discussed. The less well-known Nyquist and Nichols methods are seen as offering certain advantages and accuracy for interpreting and analyzing driver/vehicle data over the more prevalent and widely used Bode method. The effect of more extreme variations in vehicle dynamics and driver steering control characteristics on the nature of the graphical loci representing each method were illustrated using a mathematical model of the driver/vehicle system. Calculation of driver/vehicle maneuverability, as defined by an ability to track steady-state sinusoidal paths, was discussed and demonstrated for several driver control characteristics.

A principal conclusion, based upon the above analysis techniques and example calculations, is that preview-based steering control strategies as typically employed by drivers of automobiles, may produce a tradeoff of closed-loop directional stability in exchange for path maneuverability. In most cases, decreased driver preview permits

Figure 17. $F(j\omega)$, Closed-Loop Frequency Response of Path Displacement;
Influence of Driver Lag Variations.

\circ ————— \circ TP = 2.25, TAU=0.75
 \square ————— \square TP = 1.0, TAU=0.10



improved path maneuverability at the expense of reduced closed-loop system stability. Further investigation of this conclusion and related closed-loop directional performance matters are suggested through appropriate experimental testing of driver/vehicle systems. Additional experimental measurements of the driver/vehicle system, in general, and greater use of frequency domain analysis techniques for studying such data are recommended.

REFERENCES

D'Azzo, J.J. and Houpis, C.H. (1981) Linear Control System Analysis and Design, Second Edition, McGraw-Hill Book Company, New York.

James, H.M., Nichols, N.B., and Phillips, R.S. (1947) Theory of Servomechanisms, McGraw-Hill Book Company, New York.

MacAdam, C.C. (1981) "Application of an Optimal Preview Control for Simulation of Closed-Loop Automobile Driving," IEEE Transactions on Systems, Man, and Cybernetics, Vol. SMC-11, No. 6, pp. 393-399.

McRuer, D.T., et al. (1975) "Automobile Controllability - Driver/Vehicle Response for Steering Control," Technical Report, DOT HS-801 406.

McRuer, D.T., et al. (1975) "Measurement of Driver/Vehicle Multiloop Response Properties with a Single Disturbance Input," IEEE Transactions on Systems, Man, and Cybernetics, Vol. 5, No. 5.

Weir, D.H., DiMarco, R.J., and McRuer, D.T. (1977) "Evaluation and Correlation of Driver/Vehicle Data," Technical Report, DOT-HS-5-01200.